THE ROLE OF PPARγ IN KIDNEY COLLECTING-DUCT

by

Hui Zhang

A dissertation submitted to the faculty of
The University of Utah
in partial fulfillment of the requirements for the degree of

Doctor of Philosophy

Department of Physiology

The University of Utah

August 2011

The University of Utah Graduate School

STATEMENT OF DISSERTATION APPROVAL

The dissertation of **Hui Zhang**

has been approved by the following supervisory committee members:

Tianxin Yang	, Chair	**May 13, 2011** Date Approved
Mary T. Lucero	, Member	**May 13, 2011** Date Approved
Mike Michel	, Member	**May 18, 2011** Date Approved
Christof Westenfelder	, Member	**May 13, 2011** Date Approved
Noel G. Carlson	, Member	**May 13, 2011** Date Approved

and by **Francis Edward Dudek**, Chair of

the Department of **Physiology**

and by Charles A. Wight, Dean of The Graduate School.

ABSTRACT

The peroxisome proliferator-activated receptor subtype γ (PPARγ) ligands, namely the synthetic insulin-sensitizing thiazolidinedione (TZD) compounds, have demonstrated great potential in the treatment of type II diabetes. However, their clinical applicability is limited by a common and serious side effect of edema. To address the mechanism of TZD-induced edema, we generated mice with collecting duct (CD)-specific disruption of the PPARγ gene. We found that mice with CD knockout of this receptor were resistant to the rosiglitazone- (RGZ) induced increases in body weight and plasma volume expansion found in control mice expressing PPARγ in the CD. RGZ reduced urinary sodium excretion in control and not in conditional knockout mice. Furthermore, RGZ stimulated sodium transport in primary cultures of CD cells expressing PPARγ and not in cells lacking this receptor. These findings demonstrate a PPARγ-dependent pathway in regulation of sodium transport in the CD that underlies TZD-induced fluid retention. To further study the mechanism of increased fluid reabsorption in the distal nephron in response to PPARγ agonist, we performed electrophysiological studies on primary IMCD cells to investigate the involvement of ENaC in mediating TZD-induced fluid reabsorption. RGZ treatment time-dependently inhibited the activity and expression of ENaC, the major route of transcellular transport in the CD. However, RGZ treatment decreased the

transepithelial resistance. Since ENaC was suppressed, the reduction of the TER indicated that there is an alternative pathway in regulation of sodium transport in the CD that underlies TZD-induced fluid retention.

I dedicate this dissertation to

my husband, Erick, my beloved children Nicole and Nicolas and my parents

for their constant support and unconditional love.

I love you all dearly.

TABLE OF CONTENTS

ABSTRACT iii

LIST OF FIGURES viii

ACKNOWLEDGEMENTS ix

CHAPTERS

1. INTRODUCTION 1

PPARs 1
PPAR ligands 2
Renal localization and function of PPARs 4
Distinct effects of renal PPARγ on extracellular volume and blood pressure 6
Significance of the study 9
References 12

2. COLLECTING DUCT –SPECIFIC DELETION OF PEROXISOME PROLIFERATOR-ACTIVATED RECEPTOR BLOCKS THIAZOLIDINEDIONE-INDUCED FLUID RETENTION 18

Introduction 19
Methods 19
Results 21
Discussion 23
Conclusion 24
References 24

3. THE MECHANISM BY WHICH PPARγ AGONISTS INDUCED FLUID RETENTION 25

Introduction 25
Materials and methods 27
Results 31
Discussion 32

References..... 41

4. SUMMARY AND PERSPECTIVES..... 44

LIST OF FIGURES

Figure Page

2.1. Validation of CD-specific KO of PPARγ 20

2.2. Body weight gains in untreated and RGZ-treated PPARγ$^{f/f}$ and CD PPARγ KO mice 21

2.3. Changes in plasma volume in PPARγ$^{f/f}$ and CD PPARγ KO mice after RGZ treatment 21

2.4. Comparison of urinary sodium excretion and sodium intake between PPRAγ$^{f/f}$ and CD PPARγ KO mice 22

2.5. Comparison of sodium transport between the cultured CD cells derived from PPARγ$^{f/f}$ and CD PPARγ KO mice 23

3.1. Effect of RGZ on ENaC mRNA expression in renal inner medulla of wild type (WT) and CD PPARγ KO mice (KO). 36

3.2. Effect of RGZ on amiloride-sensitive Isc in primary IMCD cells 37

3.3. Effect of RGZ on ENaC mRNA expression in the IMCD cells 38

3.4. Effect of RGZ on the TER in the IMCD cells 39

ACKNOWLEDGEMENTS

First and foremost I want to thank my advisor Dr. Tianxin Yang. It has been an honor to be his first Ph.D. student. I appreciate all his contributions of time, ideas, and funding to make my Ph.D. experience productive and stimulating. The enthusiasm he has for his research was contagious and motivational for me, even during tough times in the Ph.D. pursuit. I am also thankful for the excellent example he has provided as a successful scientist and professor.

The members of the Dr. Yang's lab have contributed immensely to my personal and professional time at Utah. The lab has been a source of friendships as well as good advice and collaboration. I am especially grateful for the lab members who stuck it out in graduate school with me: Wenling Ye, Xiaohua Guo, Zhanjun Jia, Aihua Zhang, Sunny, Haiying Liu, Zachary Warnock and Tyson.

I also have to thank the members of my PhD committee, Dr. Mary T. Lucero, Dr. Mike Michel, Dr. Christof Westenfelder and Dr. Noel G. Carlson for their helpful career advice and suggestions in general.

I will forever be thankful to my department graduate advisor, Dr. Mary T. Lucero. Dr. Lucero has been helpful in providing advice many times during my graduate school career. She was and remains my best role model for a mentor and teacher. Her enthusiasm and love for students is contagious.

I also thank Vicki Anne Skelton for all the administrative help, for always being so helpful and friendly.

Lastly, I would like to thank my family for all their love and encouragement. For my parents who raised me with unconditional love and supported me in all my pursuits. For my children, Nicole and Nicolas, who give me happiness and joy all the time. And most of all for my loving, supportive and encouraging husband Erick whose faithful support during the final stages of this Ph.D. is so appreciated. Thank you.

CHAPTER 1

INTRODUCTION

PPARs

PPARs are a group of zinc finger containing transcription factors, a subfamily of the nuclear hormone receptor gene family. PPARs have four major functional domains: an NH_2-terminal ligand-independent transactivation domain (A/B domain), a DNA-binding domain (DBD; or C domain), a cofactor docking domain (D domain), and a COOH-terminal E/F domain that includes the ligand binding domain and the ligand-dependent transactivation domain (AF2 domain)(1). To date, three subtypes of PPARs have been described from several species: PPARα, β (also called d or NUC-1), and γ (2,3,4). They share a high degree of similarity in their overall amino acid sequences, particularly in the DNA binding domain (5). The three PPARs heterodimerize with retinoid X receptor (RXR) and bind to the same peroxisomal proliferator-responsive element (PPRE) in the promoter regions of their target genes and modulate gene transcription.

The function of PPARs is modified by the precise shape of their ligand-binding domain induced by ligand binding and by a number of coactivator and corepressor proteins(4,6). These coactivators and corepressor are small accessory molecules that are critical determinants of the transcriptional complex.

The coactivators include cAMP response element-binding protein (CREB), PPAR-γ coactivators(PGC-1), cAMP response element-binding protein binding protein, and steroid receptor coactivator-1. Co-repressors such as nuclear receptor co-repressor (N-CoR) and silencing mediator of retinoid acid (SMRTs1) and thyroid hormone receptor can modulate the transcriptional activity of PPAR by remodeling chromatin and establishing physical contacts with transcription initiation machinery (7,8).

PPAR ligands

PPAR ligands include endogenous and exogenous ligands (9). Endogenous ligands for the PPARs include free fatty acids and eicosanoids. PPAR*α* exhibiting the highest activity with unsaturated fatty acids, while saturated fatty acids are weak PPAR*α* ligands in general (10). Biological modifications of linoleic acid, linolenic acid, eicosapentanoic acid (EPA), and arachidonic acid originate PPAR*α* activators (10,11,12,13). Moreover, the oxidized form of EPA, eicosanoids (15-hydroxy-eicosatetranoic acid, HETE and HODEs), and leukotriene B4 had also been reported to be PPAR*α* activators (1,12,13,14,15).

PPARγ is activated by natural ligands including several prostanoids such as 15-deoxy-prostaglandin J2 (15d-PG J2) and 15-hydroxy-eicosatetranoic acid (HETE), which are metabolites of arachidonic acid (16). 15d-PG J2 (the most widely used natural ligand for PPARγ) is gamma-selective at low concentrations but also activates alpha at higher levels (17,18). Like PPARα, PPAR*β*/*δ* is activated by long chain fatty acids, including several polyunsaturated fatty acids

and eicosanoids(19). Erucic acid has been reported to be more selective for PPAR*β*/*δ* than other PPAR subtypes (20).

Synthetic ligands of PPARs have been widely used to treat various diseases. The triglyceride-lowering/high-density lipoprotein (HDL)-raising fibrates (gemfibrozil, fenofibrate, clofibrate, ciprofibrate) are PPAR*α* agonists used clinically to treat dyslipidemia (21,22). The insulin-sensitizing thiazolindinedione (TZD) class (troglitazone, pioglitazone and rosiglitazone) is PPAR*γ* activators that are used to treat diabetes mellitus (23,24). Several nonsteroidal anti-inflammatory drugs (NSAIDs), in particular indomethacin and ibuprofen, bind to PPAR*γ* and are weak PPAR*γ* agonists at high micromolar concentrations (25,26). The first PPAR*β*/*δ*-selective agonists (L-165041 and GW501516) were shown to augment HDL-C in diabetic mice as well as in obese rhesus monkeys, in which they results in normalization of metabolic parameters and reduction of fatty adiposity, which may be related to the ability of PPAR*β*/*δ* ligands to increase serum HDL levels (27,28).

Distinct functions for PPAR family members are suggested from their tissue-specific expression patterns. PPARα mRNA is mainly expressed in liver, kidney, and heart, where it controls fatty acid and lipid metabolism. PPARα-null mice exhibit higher serum levels of cholesterol and triglycerides (29) Moreover, these mice display extensive hepatic lipid accumulation and increased gonadal adipose storage and plasma FFA levels (30). PPARß expressed widely (31,32) and its function remains unclear, although recent evidence suggests a key role in fatty acid oxidation and energy uncoupling in skeletal muscle, which leads to

decreased plasma triglyceride levels, increased HDL-cholesterol concentrations, and a lean phenotype. PPARγ modulates the expression of large gene arrays in adipose tissues, where it promotes adipogenesis, decreases free fatty acid (FFA) release, improves insulin sensitivity, and attenuates. PPARγ is highly expressed in fat tissues, where it controls adipocyte differentiation, lipid storage and adipose inflammation (33).

Renal localization and function of PPARs

Under physiological conditions, all three PPAR isoforms are expressed differentially in the kidney. PPARα is mainly expressed in proximal tubules and medullary thick ascending limbs, with lower levels in glomerular mesangial cells. PARβ is ubiquitously expressed at low levels in all segments of nephron, including in glomerular mesangial cells, medullary interstitial cells, and stromal cells. PPARγ is dominantly expressed in medullary collecting ducts, pelvic urothelium and glomerular mesangial cells. The PPARγ partner RXRα has a complimentary distribution the collecting ducts (34). The differences in the distribution PPAR isoforms may result in a different role of PPAR along urinary tract.

Lots of evidence demonstrates that PPAR-alpha plays a major role in triggering fatty acid utilization and the adaptive response to dietary lipids in the kidney. One of the important pieces of evidence is found in PPAR-alpha null mice: fasting induced up-regulation of renal protein PDK4 expression was much lower than in wild type mice (35). In kidney, PPAR-beta/delta contributes to cell

survival of renal interstitial cell in medullary hyperosmality. Abundant and active PPARβ/δ was observed in cultured renal medullary interstitial cells. Overexpression of PPARβ/δ provides protection against hypertonicity-induced cell death in cultured medullary interstitial cells, which suggests that PPARβ/δ is an important survival factor in the kidney (35). An in vivo study by Letavernier et al. (36) showed that PPARβ/δ mutant mice exhibited much greater kidney dysfunction and injury than wild type. This protective effect was accompanied by a significant reduction in medullary necrosis, apoptosis, and inflammation. These findings point to reduced renal PPARβ/δ expression possibly representing an underlying mechanism involved in diabetic kidney injury. Recent studies show that PPAR-gamma involved in the normal kidney development, renal lipid metabolism, and activation of the rennin-angiotensin system. In Kidney, PPAR-gamma is mainly expressed in the distal collecting system, as its distribution pattern suggests, PPAR-gamma is involved in regulating renal hemodynamic and water and sodium transport. Furthermore, it also participates in the pathogenesis of glomerulopathy, antidiabetic thiazolidinedione-related water and sodium retention and renal, bladder and prostate carcinomas.

Distinct effects of renal PPARγ on extracellular volume and blood pressure

Renal regulation of sodium and water excretion is central to the control of blood pressure and extracellular fluid volume. Lots of evidence suggests a

potential role of renal PPARγ in regulation of salt and water excretion and blood pressure, and this evidence can be summarized in the following categories:

First of all is localization of PPARγ in the CD. Although sodium transport occurs throughout the length of the renal tubule, the fine regulation of sodium excretion occurs principally in the renal collecting duct (37). In the mouse kidney, PPARγ mRNA, determined by RT-PCR, was found to be abundant in renal inner medulla, localized to inner medullary collecting duct (IMCD) and renal medullary interstitial cells (RMIC) (38). Immunohistochemical staining of normal human kidney sections showed that PPARγ is highly expressed in the distal convoluted tubule, CCDs, and medullary CDs (39), the A6, M1, and mpkCCD_{c14} cells (40). This unique distribution pattern indicates a role of PPARγ in modulation of the CD function. The connective tubules and collective ducts are parts of the distal collecting system, where hormone-regulated ion exchange and water reabsorption takes place and provides the balance of interstitial fluid volume. If aldosterone is present, sodium is reabsorbed and potassium is secreted. Sodium transport is followed by passive water reabsorption, therefore, this mechanism regulates the total electrolytes and water volume in the body. The epithelium of the collecting ducts is responsive to antidiuretic hormone. If the hormone is present, the epithelia become permeable to water. The distal collecting system is, therefore, a major site of fluid volume regulation.

Second are reduction of urinary sodium and water excretion and blood pressure by thiazolidinediones (TZDs). Thiazolidinediones (TZDs), synthetic insulin-sensitizing drugs that include troglitazone, pioglitazone, and rosiglitazone

(RGZ), are highly effective in the treatment of type II diabetes. TZDs are believed to mediate their antidiabetic effect via activation of peroxisome proliferator-activated receptor γ(PPARγ) (41). In addition to lowering blood glucose, these drugs also benefit cardiovascular parameters, such as blood pressure and endothelial function (42,43). However, fluid retention, presented as rapid weight gain, and peripheral and pulmonary edema had emerged as the most common and serious side effects of TZDs (36). Song et al. reported that chronic three-day administration of rosiglitazone to Sprague Dawley rats significantly reduced urine volume (by 22%) and sodium excretion (by 44%) (44). These findings suggested a physiological role of PPARγ in the regulation of extracellular volume. Non-insulin-dependent diabetes mellitus with associated insulin insensitivity and reactive hyperinsulinemia is often complicated by hypertension. Increased blood pressure could in part be due to volume expansion resulting from improper avid Na^+ reabsorption by the kidney. Insulin increases Na^+ reabsorption in the distal renal nephron; likely by targeting ENaC localized to the luminal membrane of principal cells. The highest incidence of edema has been reported when TZDs are utilized in combination with insulin. Global awareness of this side effect has increased as a result of the growing number of reported cases. In a recent issue of *Circulation* (45), the American Heart Association and American Diabetes Association jointly issued a Consensus Statement commenting on the safety of TZD as related to edema.

Third is the stimulation of renal transporters by PPARγ activation. These transporters lining the renal epithelia include basolateral Na-K-ATPase, and the

following apical transporters that vary with individual nephron segments: the sodium hydrogenexchanger subtype III (NHE3) and the sodium phosphate cotransporter subtype II (NaPi-2) in the proximal convoluted tubule, the bumetanide-sensitive Na-K-2Cl cotransporter (NKCC2 or BSC1) in the thick ascending limb, the thiazide-sensitive Na-Cl cotransporter (NCC or TSC) in the distal convoluted tubule, and the amiloride-sensitive sodium channel (ENaC) in the collecting duct. The major water channel proteins (aquaporins, AQPs) in the kidney include AQP1-4, of which AQP1 and AQP2 function on the apical membrane, and AQP3 and AQP4 on the basolateral membrane (46). PPARγ activation by rosiglitazone in Sprague-Dawley rats increases protein abundance of various transporters, including the α-1 subunit of Na-K-ATPase, the bumetanide-sensitive Na-K-2Cl cotransporter (NKCC2), the aquaporins 2 (AQP2) and 3 (AQP3) and the sodium hydrogen exchanger (NHE3) (44). *In vitro* studies show that activation of PPARγ enhances ENaC abundance in the apical membrane of cultured CD cells (47).

In contrast to the fluid retaining and prohypertensive effect of renal PPARγ, vascular PPARγ has been implicated to exert anti-hypertensive action. PPARγ is expressed in vascular system (47), such as in endothelial cells (48,49), vascular smooth muscle cells (VSMC) (50) and monocyte/macrophages (51,52,53). PPARγ activators rosiglitazone and pioglitazone prevent hypertension in Ang II-infused rats and abrogate the structural, functional changes induced by Ang II in blood vessels (54). Rosiglitazone also lowers blood pressure in normotensive rats and this is incompatible with enhanced fluid retention in these

animals (44), suggesting that the reduction of blood pressure may be attributed to the activation of PPARγ in vasculature but not in the kidney.

Significance of the study

The mechanisms of fluid retention in patients treated with TZDs are not fully understood and may involve a number of factors, including reduction of urinary sodium excretion (2), alteration of endothelial permeability (37), increased sympathetic nervous system activity (40), or altered interstitial ion transport (20). We hypothesize that activation of PPARγ in the distal nephron may serve as the primary mechanism responsible for TZD-induced fluid retention. To evaluate a role of PPARγ in fluid retention, we built a mouse model with disrupted PPARγ specifically in the collecting ducts (CDs) in the kidney. We found that mice with CD-specific knockout of PPARγ were resistant to the rosiglitazone-induced increase in body weight and rosiglitazone stimulated sodium transport in primary cultures of CDs cells expressing PPARγ but not in cells lacking this receptor (55). Our results were impressively complemented by the study of Guan et al. (56), which investigated the effects of pioglitazone and amiloride on weight gain and sodium retention again in knockout mice and in collecting-duct cellculture. Similarly, they found that deletion of CD PPARγ decreased renal Na+ avidity and increased plasma aldosterone. Mice treated with TZDs experience early weight gain from increased total body water. Moreover, weight gain was blocked by the diuretic amiloride. The similar effects of rosiglitazone and pioglitazone illustrate that stimulation of sodium transport in the collecting duct is a class effect of

glitazones, and proved our hypothesis that the activation of PPARγ in the distal nephron is the primary mechanism responsible for TZD-induced fluid retention.

The PPARγ is reported to regulate SGK1, a protein kinase that is known as a key regulator of ENaC (58). PPARγ agonists have been shown to stimulate the transcription of the SGK1, which might enhance the surface expression of ENaC(39). The results suggested that PPARγ activators may increase renal Na+ reabsorption by stimulating ENaC and Serum- and Glucocorticoid-Regulated Kinase 1 (SGK1). It is believed that SGK1 expression is induced by aldosterone and then stimulates ENaC activity. In human CCD cells, SGK1 activity is stimulated by treatment with PPARγ agonists. An increase in SGK1 mRNA may lead to increased levels of cell surface ENaCα (39).

However, increasing evidence has shown contradictory results indicating the failure of PPARγ agonists to affect ENaC activity. Nofziger et al.(2005) demonstrated that two PPARγ agonists, pioglitazone and GW7845, did not directly enhance basal or insulin-stimulated Na^+ transport via ENaC in the A6, M-1, and mpkCCD_{c14} cell lines. In addition, Vallon et al. recently published a study using mice with CD-specific conditionally inactivated αENaC (59) and patch-clamp experiments in wild-type mice to assess the effect of PPARγ agonists on ENaC activity in isolated CD (60). The authors proposed that TZD-induced fluid retention and weight gain are mediated by nonselective cation channels in inner medullary CD, and ENaC-mediated Na^+ reabsorption in the CD is not critical for this effect. To further study the exact mechanism of TZD caused excess sodium retention, we performed electrophysiological studies on primary cultures of inner

medullary collecting duct (IMCD) cells to evaluate mechanisms of rosiglitazone (RGZ)-stimulated ion transport.

References

1. Guan Y. Peroxisome proliferator-activated receptor family and its relationship to renal complications of the metabolic syndrome. *J Am Soc Nephrol* .2004; 15: 2801–2815.

2. Keller H, Mahfoudi A, Dreyer C, Hihi AK, Medin J, Ozato K, and Wahli W. Peroxisome proliferator-activated receptors and lipid metabolism. *Ann N Y Acad Sci* .1993; 684: 157-173.

3. Mangelsdorf DJ, Thummel C, Beato M, Herrlich P, Schutz G, Umesono K, Blumberg B, Kastner P, Mark M, Chambon P,et al. The nuclear receptor superfamily: the second decade. *Cell* .1995; 83: 835-839.

4. Schoonjans K, Staels B, and Auwerx J. The peroxisome proliferator activated receptors (PPARS) and their effects on lipid metabolism and adipocyte differentiation. *Biochim Biophys Acta* .1996; 1302: 93-109.

5. Gross V, Schneider W, Schunck WH, Mervaala E, and Luft FC. Chronic effects of lovastatin and bezafibrate on cortical and medullary hemodynamics in deoxycorticosterone acetate-salt hypertensive mice. *J Am Soc Nephrol*.1999; 10: 1430-1439.

6. Nielsen S, DiGiovanni SR, Christensen EI, Knepper MA, and Harris HW. Cellular and subcellular immunolocalization of vasopressin-regulated water channel in rat kidney. *Proc Natl Acad Sci U S A* .1993; 90: 11663-11667.

7. Desvergene B and Wahli W. Peroxisome proliferator-activated receptor: nuclear control of metabolism. *Endocr Rev* .1999; 20: 649–688.

8. Qi C, Zhu Y and Reddy JK. Peroxisome proliferator-activated receptors, coactivators, and downstream targets. *Cell Biochem Biophys*.2000; 32: 187–204.

9. Willson TM. and Wahli W. Peroxisome proliferator-activated receptor agonists. *Curr Opin Chem Biol.* 1997; 1(2):235-41

10. Ahmed W, Ziouzenkova O, Brown J, Devchand P, Francis S, Kadakia M, Kanda T, Orasanu G, Shariach M, Aandbergen F, and Plutzky J. PPARs and their metabolic modulation: new mechanisms for transcriptional regulation? *J of Internl Med.* 2007; 262(2): 184–198.

11. Krey G, Braissant O, L'Horset F, Kalkhoven E, Perroud M, Parker MG, and Wahli W.. Fatty acids, eicosanoids, and hypolipidemic agents identified as ligands of peroxisome proliferator-activated receptors by

coactivator-dependent receptor ligand assay. *Mol Endocrinol.* 1997; 11(6):779–791.

12. Kliewer SA, Sundseth SS, Jones SA, Brown PJ, Wisely GB, Koble CS, Devchand P, Wahli W, Willson TM, Lenhard JM and Lehmann JM. Fatty acids and eicosanoids regulate gene expression through direct interactions with peroxisome proliferator-activated receptors α and γ . *Proc Natl Acad Sci U S A* . 1997; 94(9): 4318–432364.

13. Forman BM, Chen J, and Evans RM. Hypolipidemic drugs, polyunsaturated fatty acids, and eicosanoids are ligands for peroxisome proliferator-activated receptors α and δ . *Proc Natl Acad Sci U S A* .1997; 94(9):4312–4317.

14. Devchand PR, Keller H, Peters JM, Vazquez M, Gonzalez FJ and Wahli W. The PPARα-leukotriene B4 pathway to inflammation control. *Nature*. 1996; 384(6604):39–43.

15. Sethi S, Ziouzenkova O, Ni H, Wagner DD, Plutzky J and Mayadas TN. Oxidized omega-3 fatty acids in fish oil inhibit leukocyte-endothelial interactions through activation of PPARα . *Blood.* 2002;100(4):1340–1346.

16. Theocharis S, Margeli A, Vielh P and Kouraklis G. Peroxisome proliferator-activated receptor-γ ligands as cell-cycle modulators. *Cancer Treat Rev.* 2004; 30(6):545–554.

17. Kliewer SA, Lenhard JM, Willson TM, Patel I, Morris DC and Lehmann JM. A prostaglandin J2 metabolite binds peroxisome proliferator-activated receptor γ and promotes adipocyte differentiation. *Cell.* 1995;83(5):813–819.

18. Komar CM. Peroxisome proliferator-activated receptors (PPARs) and ovarian function—implications for regulating steroidogenesis, differentiation, and tissue remodeling. *Reprod Bioly Endocrinol..* 2005;3: 41

19. Willson TM, Brown PJ, Sternbach DD and Henke BR. The PPARs: from orphan receptors to drug discovery. *J of Med Chem*. 2000; 43(4):527–550

20. Brown JD and Plutzky J. Peroxisome proliferator-activated receptors as transcriptional nodal points and therapeutic targets. *Circulation.* 2007; 115(4):518–533

21. Forman BM, Chen J and Evans RM. The peroxisome proliferator-activated receptors: ligands and activators. *Annals of the New York Academy of Sciences.* 1996; 804:266–275.

22. Staels B and Fruchart J-C. Therapeutic roles of peroxisome proliferator-activated receptor agonists. *Diabetes.* 2005;54(8):2460–2470.

23. Lehmann JM, Moore LB, Smith-Oliver TA, Wilkison WO, Willson TM and Kliewer SA. An antidiabetic thiazolidinedione is a high affinity ligand for peroxisome proliferator-activated receptor γ (PPARγ). *J Biol Chem .* 1995; 270(22):12953–12956.

24. Lehrke M and Lazar MA. The many faces of PPARγ. *Cell.* 2005; 123(6):993–999.

25. Lehmann JM, Lenhard JM, Oliver BB, Ringold GM and Kliewer SA. Peroxisome proliferator-activated receptors α and γ are activated by indomethacin and other non-steroidal anti-inflammatory drugs. *J Biol Chem .* 1997; 272(6):3406–341076.

26. Adamson DJA, Frew D, Tatoud R, Wolf CR and Palmer CNA. Diclofenac antagonizes peroxisome proliferator-activated receptor-γ signaling. *Mol Pharmacoy.* 2002; 61(1):7–12.

27. Leibowitz MD, Fiévet C, Hennuyer N, et al. Activation of PPARδ alters lipid metabolism in db/db mice. *FEBS Letters*. 2000; 473(3):333–336.

28. Oliver WR, Jr., Shenk JL, Snaith MR, et al. A selective peroxisome proliferator-activated receptor δ agonist promotes reverse cholesterol transport. *Proc Natl Acad Sci U S A* 2001; 98(9):5306–5311.

29. Akiyama TE, Nicol CJ, Fievet C, Staels B, Ward JM, Auwerx J, Lee SS, Gonzalez FJ and Peters JM. Peroxisome proliferator-activated receptor-alpha regulates lipid homeostasis, but is not associated with obesity: studies with congenic mouse lines. *J Biol Chem* .2001; 276: 39088–39093.

30. Leone TC, Weinheimer CJ and Kelly DP. A critical role for the peroxisome proliferator-activated receptor alpha (PPARalpha) in the cellular fasting response: the PPARalpha-null mouse as a model of fatty acid oxidation disorders. *Proc Natl Acad Sci USA* .1999; 96: 7473–7478.

31. Braissant O, Foufelle F, Scotto C, Dauca M, and Wahli W. Differential expression of peroxisome proliferator-activated receptors (PPARs): tissue distribution of PPAR-alpha, -beta, and -gamma in the adult rat. *Endocrinology* .1996;137: 354-366.

32. Kliewer SA, Forman BM, Blumberg B, Ong ES, Borgmeyer U, Mangelsdorf DJ, Umesono K, and Evans RM. Differential expression and

activation of a family of murine peroxisome proliferator-activated receptors. *Proc Natl Acad Sci U S A* .1994; 91: 7355-7359.

33. Xiongzhong Ruan, Feng Zheng, and Youfei Guan. PPARs and the kidney in metabolic syndrome. *Am. J. Physiol Renal Physiol.* 2008; 294: F1032-F1047

34. Guan Y, Zhang Y, Davis L and Breyer MD. Expression of peroxisome proliferator-activated receptors in urinary tract of rabbits and humans. *Am J Physiol Renal Physiol* .1997; 273: F1013–F1022, 1997

35. Leone TC, Weinheimer CJ and Kelly DP. A critical role for the peroxisome proliferator-activated receptor alpha (PPARalpha) in the cellular fasting response: the PPARalpha-null mouse as a model of fatty acid oxidation disorders. *Proc Natl Acad Sci USA* ;1999; 96: 7473–7478.

36. Hao CM, Redha R, Morrow J and Breyer MD. Peroxisome proliferator-activated receptor delta activation promotes cell survival following hypertonic stress. *J Biol Chem* 277: 21341–21345

37. Letavernier E, Perez J, Joye E, Bellocq A, Fouqueray B, Haymann JP, Heudes D, Wahli W, Desvergne B and Baud L. Peroxisome proliferator-activated receptor beta/delta exerts a strong protection from ischemic acute renal failure. *J Am Soc Nephrol* .2005; 16: 2395–2402.

38. Yang T, Michele DE, Park J, Smart AM, Lin Z, Brosius FC, Schnermann JB and Briggs JP. Expression of peroxisomal proliferator-activated receptors and retinoid X receptors in the kidney. *Am J Physiol*.1999;277:F966–F973.

39. Hong G, Lockhart A, Davis B, Rahmoune H, Baker S, Ye L, Thompson P, Shou Y, O'Shaughnessy K, Ronco P, et al. PPARgamma activation enhances cell surface ENaCalpha via up-regulation of SGK1 in human collecting duct cells. *FASEB J* .2003; 17:1966–1968.

40. Nofziger C, Chen L, Shane MA, Smith CD, Brown KK and Blazer-Yost BL PPARgamma agonists do not directly enhance basal or insulin-stimulated Na+ transport via the epithelial Na+ channel. *Pflugers Arch.*2005; 451:445–453.

41. Cheng-Lai, A. and Levine, A. Rosiglitazone: an agent from the thiazolidinedione class for the treatment of type 2 diabetes. *Heart Dis*. 2000;2:326-333.

42. Haffner, S. M., Greenberg, A. S., Weston, W. M., Chen, H., Williams and K. & Freed, M. I. Effect of rosiglitazone treatment on nontraditional

markers of cardiovascular disease in patients with type 2 diabetes mellitus. *Circulation* .2002;106: 679-684.

43. Parulkar, A. A., Pendergrass, M. L., Granda-Ayala, R., Lee, T. R. and Fonseca, V. A. Nonhypoglycemic Effects of thiazolidinediones, *Ann. Intern. Med.* 2001;134: 61-71.

44. Song J, Knepper MA, Hu X, Verbalis JG, and Ecelbarger CA. Rosiglitazone activates renal sodium- and water-reabsorptive pathways and lowers blood pressure in normal rats. *J Pharmacol Exp Ther.*2004 308: 426-433.

45. Nesto, R. W., Bell, D., Bonow, R. O., Fonseca, V., Grundy, S. M., Horton, E. S., Le Winter, M., Porte, D., Semenkovich, C. F., Smith, S., et al. Thiazolidinedione use, fluid retention, and congestive heart failure. *Circulation* 2003;108:2941-2948.

46. Yang T. and Soodvilai S. Renal and vascular mechanisms of thiazolidinedione-induced fluid retention. *PPAR Research.* 2008; 2008:943614

47. Bishop-Bailey D. Peroxisome proliferator-activated receptors in the cardiovascular system. *Br J Pharmacol* .2000;129: 823-834.

48. Inoue I, Shino K, Noji S, Awata T, and Katayama S. Expression of peroxisome proliferator-activated receptor alpha (PPAR alpha) in primary cultures of human vascular endothelial cells. *Biochem Biophys Res Commun*.1998; 246: 370-374.

49. Satoh H, Tsukamoto K, Hashimoto Y, Hashimoto N, Togo M, Hara M, Maekawa H, Isoo N, Kimura S, and Watanabe T. Thiazolidinediones suppress endothelin-1 secretion from bovine vascular endothelial cells: a new possible role of PPARgamma on vascular endothelial function. *Biochem Biophys Res Commun*,1999; 254: 757-763.

50. Staels B, Koenig W, Habib A, Merval R, Lebret M, Torra IP, Delerive P, Fadel A, Chinetti G, Fruchart JC, Najib J, Maclouf J, and Tedgui A. Activation of human aortic smooth-muscle cells is inhibited by PPARalpha but not by PPARgamma activators. *Nature.*1998;393: 790-793.

51. Chinetti G, Griglio S, Antonucci M, Torra IP, Delerive P, Majd Z, Fruchart JC, Chapman J, Najib J, and Staels B. Activation of proliferator-activated receptors alpha and gamma induces apoptosis of human monocyte-derived macrophages. *J Biol Chem* .1998; 273: 25573-25580.

52. Parulkar, A. A., Pendergrass, M. L., Granda-Ayala, R., Lee, T. R. and Fonseca, V. A. Nonhypoglycemic effects of thiazolidinediones Ann. Intern. *Med.* 2001;134, 61-71.

53. Ricote M, Li AC, Willson TM, Kelly CJ, and Glass CK. The peroxisome proliferator-activated receptor-gamma is a negative regulator of macrophage activation. *Nature* .1998;391: 79-82.

54. Diep QN, El Mabrouk M, Cohn JS, Endemann D, Amiri F, Virdis A, Neves MF, and Schiffrin EL. Structure, endothelial function, cell growth, and inflammation in blood vessels of angiotensin II-infused rats: role of peroxisome proliferator-activated receptor-gamma. *Circulation*.2002; 105: 2296-2302.

55. Zhang H, Zhang A, Kohan D. E, Nelson RD,Gonzalez FJ, and Yang T. , Collecting duct-specific deletion of peroxisome proliferator-activated receptor γ blocks thiazolidinedione- induced fluid retention. Proc Natl Acad Sci U S A 2005; 102: 9406–9411.

56. Guan Y, Hao C, Cha D. R, Lu W, Kohn DE, Magnuson MA, Redha R, Zhang and Y, Breyer MD. Thiazolidinediones expand body fluid volume through PPARγ stimulation of ENaC-mediated renal salt absorption. *Nature Medicine*.2005; 11(8): 861–866.

57. Chen SY, Bhargava A, Mastroberardino L, Meijer OC, Wang J, Buse P, Firestone GL, Verrey F and Pearce D. Epithelial sodium channel regulated by aldosterone-induced protein Sgk. *Proc Natl Acad Sci U S A* 1999;96:2514–2519

58. Nofziger C, Chen L, Shane MA, Smith CD, Brown KK and Blazer-Yost BL PPARgamma agonists do not directly enhance basal or insulin-stimulated Na+ transport via the epithelial Na+ channel. *Pflugers Arch* 2005; 451:445–453.

59. Rubera I, Loffing J, Palmer LG, Frindt G, Fowler-Jaeger N, Sauter D, Carroll T, McMahon A, Hummler E and Rossier BC. Collecting duct-specific gene inactivation of alphaENaC in the mouse kidney does not impair sodium and potassium balance. *J Clin Invest.* 2003;112:554–565.

60. Vallon V, Hummler E, Rieg T, Pochynyuk O, Bugaj V, Schroth J, Dechenes G, Rossier B, Cunard R and Stockand J . Thiazolidinedione-induced fluid retention is independent of collecting duct alphaENaC activity. *J Am Soc Nephrol*. 2009;20:721–729.

CHAPTER 2

COLLECTING DUCT –SPECIFIC DELETION OF PEROXISOME PROLIFERATOR-ACTIVATED RECEPTOR BLOCKS THIAZOLIDINEDIONE-INDUCED FLUID RETENTION

Collecting duct-specific deletion of peroxisome proliferator-activated receptor γ blocks thiazolidinedione-induced fluid retention

Hui Zhang*†‡, Aihua Zhang*†‡, Donald E. Kohan*, Raoul D. Nelson§, Frank J. Gonzalez¶, and Tianxin Yang*†‖

Departments of *Internal Medicine and §Pediatrics, University of Utah, Salt Lake City, UT 84132; †Salt Lake Veterans Affairs Medical Center, Salt Lake City, UT 84148; and ¶National Cancer Institute, National Institutes of Health, Bethesda, MD 20892

Edited by Maurice B. Burg, National Institutes of Health, Bethesda, MD, and approved May 19, 2005 (received for review March 2, 2005)

The peroxisome proliferator-activated receptor subtype γ (PPARγ) ligands, namely the synthetic insulin-sensitizing thiazolidinedione (TZD) compounds, have demonstrated great potential in the treatment of type II diabetes. However, their clinical applicability is limited by a common and serious side effect of edema. To address the mechanism of TZD-induced edema, we generated mice with collecting duct (CD)-specific disruption of the PPARγ gene. We found that mice with CD knockout of this receptor were resistant to the rosiglitazone- (RGZ) induced increases in body weight and plasma volume expansion found in control mice expressing PPARγ in the CD. RGZ reduced urinary sodium excretion in control and not in conditional knockout mice. Furthermore, RGZ stimulated sodium transport in primary cultures of CD cells expressing PPARγ and not in cells lacking this receptor. These findings demonstrate a PPARγ-dependent pathway in regulation of sodium transport in the CD that underlies TZD-induced fluid retention.

roziglitazone | Cre recombinase | Evans blue technique

Thiazolidinediones (TZDs), synthetic insulin-sensitizing drugs that include troglitazone, pioglitazone, and rosiglitazone (RGZ), are highly effective in the treatment of type II diabetes. TZDs are believed to mediate their antidiabetic effect via activation of peroxisome proliferator-activated receptor γ (PPARγ) (1). In addition to lowering blood glucose, these drugs also benefit cardiovascular parameters, such as blood pressure and endothelial function (2, 3). However, fluid retention, presented as rapid weight gain, and peripheral and pulmonary edema have emerged as the most common and serious side effects of TZDs (4–6). Global awareness of this side effect has increased as a result of the growing number of reported cases. In a recent issue of *Circulation* (7), the American Heart Association and American Diabetes Association jointly issued a Consensus Statement commenting on the safety of TZD as related to edema. The mechanisms of fluid retention in patients treated with TZDs are poorly understood and may involve a number of factors, including reduction of urinary sodium excretion (8), alteration of endothelial permeability (9), increased sympathetic nervous system activity (10), or altered interstitial ion transport (11). To evaluate the relative contributions of these individual mechanisms, tissue- or cell-type-specific approaches are needed in carefully designed studies.

PPARs are a group of zinc finger-containing transcription factors, representing a family of the nuclear hormone receptor gene superfamily. To date, three subtypes of PPARs encoded by different genes have been described from several species: PPARα, -β/δ, and -γ (12, 13). They share a high degree of similarity in their overall amino acid sequences, particularly in the DNA-binding domain (14). The three isoforms of the PPARs heterodimerize with retinoid X receptor, bind to the same peroxisome proliferator-responsive element in the promoter regions of their target genes, and modulate gene transcription (13). Distinct functions for PPAR family members are suggested from their tissue-specific expression patterns: PPARα is mainly expressed in liver, kidney, and heart, where it controls fatty acid and lipid metabolism; PPARγ is highly expressed in fat tissues, where it controls adipocyte differentiation and lipid storage; and PPARδ is widely (15) expressed and its function largely remains unclear, although recent evidence suggests a role in fatty acid and lipid metabolism (16).

Within the kidney, PPARγ is predominantly expressed in the inner medulla and in the inner medullary collecting duct (CD) (17, 18), a critical site for the control of fluid metabolism. Therefore, we hypothesize that activation of PPARγ in the distal nephron may serve as the primary mechanism responsible for TZD-induced fluid retention. To examine this hypothesis, the present study uses the Cre-loxP system to generate mice with CD-specific deletion of PPARγ. The CD PPARγ knockout (KO) mice were generated by genetic cross between PPARγ floxed mice and transgenic mice expressing Cre recombinase under the control of the mouse AQP2 promoter. We report that TZD-induced fluid retention is remarkably blocked in CD PPARγ KO mice as compared with controls.

Methods

Transgenic Mice. We generated mice with CD-specific KO of the PPARγ gene by genetic cross between PPARγ floxed mice and AQP2-Cre mice. The PPARγ floxed mice contain two loxP sites inserted into introns 1 and 2 of the PPARγ gene flanking the critical exon 2 by homologous recombination in ES cells (19). AQP2-Cre mice contain a transgene, with 11 kb of the mouse AQP2 gene 5′ flanking region driving expression of the Cre recombinase (20). Both PPARγ floxed and AQP2-Cre mice were phenotypically normal. Homozygous PPARγ floxed (PPAR$\gamma^{f/f}$) mice were mated with female AQP2-Cre mice to yield mice heterozygous for floxed PPARγ and heterozygous for AQP2-Cre. These mice were bred with mice homozygous for floxed PPARγ to obtain mice homozygous for floxed PPARγ (termed CD PPARγ KO).

All animal procedures were approved by the University of Utah Institutional Animal Care and Use Committee.

Genotyping. The genotype of the AQP2-Cre mice was performed as described (20). Genotyping the PPARγ gene involved the use of primers PPARγ F1 (5′-CTCCAATGTTCTCAAACTTAC-3′) and PPARγ R1 (5′-GAT GAGTCATGTAAGTTGACC-3′), which yielded a 225-bp band from the wild-type allele and a 275-bp band from the floxed allele. The DNA recombination was assessed in both kidney regions and microdissected nephron segments. Renal cortex and inner medulla from CD PPARγ KO and PPAR$\gamma^{f/f}$ mice were dissected and subjected to DNA extraction by using TRIzol reagent. The DNA was amplified by using primers PPARγ F2 (5′-GACAGCACAACA ATGTTCCCA-3′) and

This paper was submitted directly (Track II) to the PNAS office.

Abbreviations: TZD, thiazolidinedione; PPARγ, peroxisome proliferator-activated receptor γ; CD, collecting duct; KO, knockout; Hct, hematocrit; RGZ, rosiglitazone; ENaC, epithelial sodium channel.

‡H.Z. and A.Z. contributed equally to this work.

‖To whom correspondence should be addressed. E-mail: tanxin.yang@hsc.utah.edu.

www.pnas.org/cgi/doi/10.1073/pnas.0501744102

Table 1. Routine physiological data

	PPARγ$^{f/f}$		CD PPARγ KO	
	Vehicle (n = 4)	RGZ (n = 5)	Vehicle (n = 4)	RGZ (n = 4)
Plasma Na, mmol/l	157 ± 0.95	162 ± 3.15	158 ± 1.65	162 ± 1.33
Plasma K, mmol/l	4.08 ± 0.1	4.55 ± 0.36	3.9 ± 0.17	4.2 ± 0.03
Plasma Cl, mmol/l	109 ± 0.91	112 ± 2.84	109 ± 2.40	113 ± 0.67
Plasma creatinine, mg/dl	1.02 ± 0.06	0.9 ± 0.04	0.95 ± 0.028	1 ± 0.00
Plasma BUN, mg/dl	27 ± 3.24	29 ± 2.86	26 ± 1.87	26 ± 3.21
Urine volume, μl/24 hr	1625 ± 188.68	1,749 ± 257.11	1,904 ± 199.27	1,762 ± 152.46
Urine creatinine, mg/dl	20.33 ± 3.60	25.5 ± 4.69	21.75 ± 1.15	19.6 ± 1.63
ClCr, ml/min	0.22 ± 0.02	0.30 ± 0.02	0.30 ± 0.05	0.25 ± 0.05
SBP, mmHg	112.67 ± 4.67	107.50 ± 2.75	123.50 ± 7.77	117.25 ± 6.85

ClCr, creatinine clearance; SBP, systolic blood pressure. No statistical significance was found between any groups.

PPARγ R2 (5′-GTATTCTATGGCTTCCAGTGC-3′), which flanked the loxP sites and yielded a 2,423-bp band from the floxed allele and a 438-bp band from the recombined allele. To evaluate the CD-specific recombination event, CD PPARγ KO mice were anesthetized by isoflurance, and the left kidney was perfused with DMEM containing 2 mg/ml each collagenase Type 1 (Worthington) and hyaluronidase (Sigma). Kidney slices were incubated in the same solution for 45 min at 37°C. Under a stereomicroscope, 20–30 of each of the following nephron segments, including glomerulus, proximal convoluted tubule, cortical and medullary thick ascending limb, cortical and inner medullary CD, were dissected. The recombined allele from the microdissected nephron segments was detected as a 438-bp band by using primers PPARγ F2 and PPARγ R2 and the floxed allele as a 1,419-bp band by using primers PPARγ F3 (5′-CTCCAATGT TCTCAA ACTTAC-3′) and PPARγ R3 (5′-CATGAACTCCATAGTGGA AGCC-3′). Because PPARγ R3 was positioned within the loxP sites, no band was detected from recombined allele by using PPARγ F3 and PPARγ R3.

RGZ Treatment and Metabolic Studies. RGZ was incorporated into a chow-based diet (LabDiet Rodent Chow 5001; Purina) at a level of 320 mg/kg diet. RGZ was made by GlaxoSmithKline and purchased from the University of Utah Hospital. The gelled diets were made by melting agar (1% by weight) in water (65%), cooling, and adding the drug (0.1%), ground chow (33.9%), and NaCl (0.5%). The final content of NaCl became 0.8%. The same gelled diets without the drug served as controls. Adult PPARγ$^{f/f}$ and CD PPARγ KO mice (3~4-month-old) were acclimatized to metabolic cages (Hatteras Instruments, Cary, NC) and the control diet for 7 days. The numbers of males and females were roughly even in each group. After the 7-day acclimation period, PPARγ$^{f/f}$ and CD PPARγ KO mice were placed on the gelled diet with or without RGZ for 9 days. Measurements of body weight and collection of 24-hour urine were performed. Hematocrit (Hct) was measured before and after RGZ treatment; at the end of experiments, plasma volume and blood pressure were determined as described in the following.

Measurement of Hct. The sphenous vein was punctured by using a #23-gauge needle, and one drop of blood (≈5–10 μl) was collected by using a 10-μl capillary glass (Idaho Technology, Salt Lake City). One side of the tube was sealed with Hemato-Seal and then centrifuged for 4 min in a Thermo IEC (Boston) microcentrifuge machine.

Measurements of Plasma Volume and Blood Pressure. Under general anesthetization with isoflurane (2 ml/min), catheters were placed in the carotid artery for direct measurement of systolic blood pressure and in the jugular vein for infusion of Evans blue. Blood pressure was recorded by using a pressure transducer (Abbott Critical Care System) and a data acquisition system (Dataq Instruments, Akron, OH). After recording of blood pressure for 5 min, 25 μl of 2 mg/ml Evans blue was injected via jugular vein catheterization. Seven minutes later, ≈700–800 μl of blood was with-

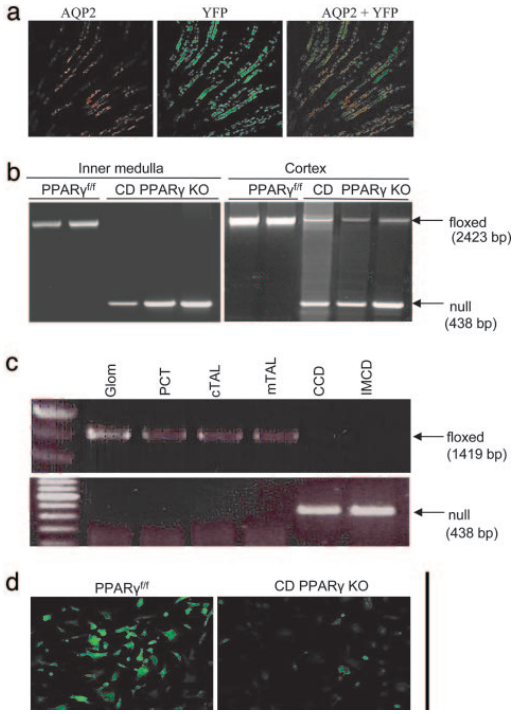

Fig. 1. Validation of CD-specific KO of PPARγ. (*a*) Colocalization of YFP expression and AQP2 immunofluorescence in mice doubly heterozygous for ROSA26-YFP and AQP2-Cre. A representative photomicrograph is shown from three separate animals (×600). (*b*) PCR analysis of AQP2-Cre mediated recombination of the PPARγ gene in the inner medulla and cortex. Null band (438 bp) is the recombination product after deletion of exon 2 of the PPARγ. Exon 2 was nearly completely deleted in the inner medulla and partially deleted in the cortex of CD PPARγ KO mice (n = 3) as compared with the floxed controls (n = 2). (*c*) PCR analysis of AQP2-Cre-mediated recombination of the PPARγ gene in microdissected nephron segments from PPARγ KO mice. (*d*) Immunocytochemistry analysis of PPARγ protein expression in CD cells derived from PPARγ KO mice. CD cells were isolated by using lectin-coated dynabeads and grown in a chamber slide. Immunocytochemistry was performed by using a polyclonal antibody against PPARγ. Shown is a representative from three separate experiments.

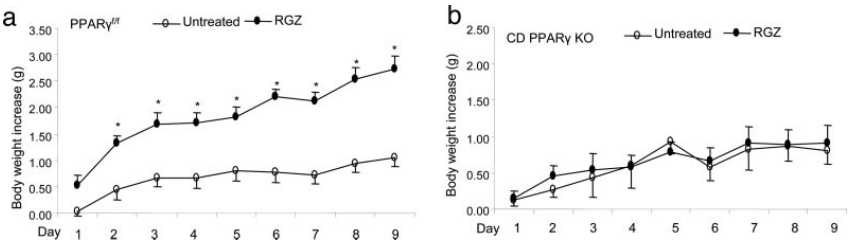

Fig. 2. Body-weight gains in untreated and RGZ-treated PPARγ$^{f/f}$ mice (*a*) and CD PPARγ KO mice (*b*). PPARγ$^{f/f}$ per vehicle, $n = 11$; PPARγ$^{f/f}$ per RGZ, $n = 9$; CD PPARγ KO per vehicle, $n = 8$; CD PPARγ KO group, $n = 9$. *, $P < 0.05$ vs. vehicle at the corresponding time point.

drawn from the vena cava by using a heparin-coated 1-cc syringe with bent #23-gauge needle. Plasma was separated by centrifugation of the blood at 5,000 × *g* for 4 min. Absorbance was read at 620 nm, and plasma Evans blue concentrations were calculated according to a standard curve generated by a serial dilution of the 2 mg/ml Evans blue-saline solution. Plasma volume was calculated by using the dilution factors of Evans blue.

Aldosterone RIA. Plasma aldosterone concentrations were determined by using Coat-A-Count RIA kit (Diagnostic Products, Los Angeles). Twenty microliters of plasma was diluted with 100 μl of diluent before the assay.

Primary Cultures of CD Cells and Measurements of Sodium Transport. The primary cultures of CD cells derived from the whole kidneys of PPARγ$^{f/f}$ and CD PPARγ KO mice were performed by using lectin-coated Dynabeads, as described (21).

For measurements of sodium transport, the CD cells were subcultured onto permeable filter supports (0.4-μm pore size, 1.13-cm^2 surface area; Transwell, Corning Costar). Cells were kept on filters for at least 10 days until a confluent transporting cell monolayer had developed. This was evaluated by measurement of the [^{14}C]-inulin leak, as described (22). Transepithelial resistance was determined by using "chopstick" electrodes (EVOM, World Precision Instruments, Sarasota, FL). Transepithelial transport of ^{22}Na was determined by adding 10 μCi (1 Ci = 37 GBq) of ^{22}Na to the apical compartment followed by measurement of the radioactivity in the basal compartment. All studies described in this report were performed on cells between the third and fifth passages.

Statistical Analysis. Values shown represent means ±SE. Statistical analysis was performed by unpaired *t* tests or ANOVA and Bonferroni tests, with a *P* value of <0.05 being considered statistically significant.

Results

Generation of Mice with CD-Specific KO of PPARγ. The PPARγ floxed mice, containing two loxP sites inserted into introns 1 and 2 of the PPARγ gene flanking the critical exon 2, were generated by homologous recombination in ES cells (19). AQP2-Cre transgenic mice expressing Cre under the control of mouse AQP2 promoter (20) were used to produce a CD-specific disruption of the PPARγ gene. To assess CreTag activity *in vivo*, AQP2-Cre mice were bred with reporter mice (ROSA26-YFP). YFP expression was restricted to kidney and testes but not other tissues examined, including lung, brain, heart, muscle, intestine, stomach, spleen, and liver (data not shown). In the kidney, YFP expression was found in AQP2-expressing CD cells (Fig. 1*a*). Homozygous PPARγ floxed (PPARγ$^{f/f}$) mice were mated with female AQP2-Cre mice to yield mice heterozygous for the floxed PPARγ allele and heterozygous for the AQP2-Cre transgene. These mice were bred with mice homozygous for the floxed PPARγ to obtain mice homozygous for the floxed PPARγ (termed CD PPARγ KO). CD PPARγ KO mice had no gross morphological abnormalities until at least 6 months of age.

The 438-bp products derived from the recombined allele were detected in both the inner medulla and cortex of CD PPARγ KO mice but not in those of PPAR$^{f/f}$ mice (Fig. 1*b*). The 2,423-bp products derived from the floxed allele were almost undetectable in the inner medulla and were substantially reduced in the renal cortex of CD PPARγ KO mice, compared with the floxed controls. To confirm the CD-specific recombination, microdissected nephron segments from CD PPARγ KO mice were examined for the existence of the floxed and recombined alleles. The recombined allele, detected as a 438-bp band, was found only in the CD (cortical and inner medullary CDs) but not in other segments; the floxed

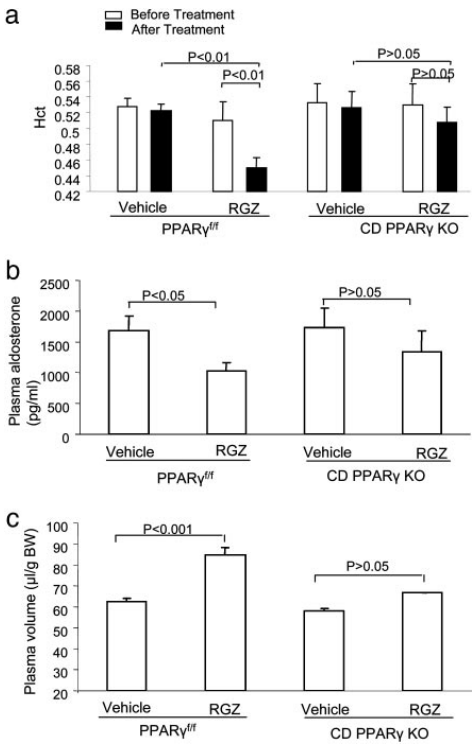

Fig. 3. Changes in plasma volume in PPARγ$^{f/f}$ and CD PPARγ KO mice after RGZ treatment. (*a*) Hct in PPARγ$^{f/f}$ and CD PPARγ KO mice before and after RGZ treatment. PPARγ$^{f/f}$ per vehicle, $n = 4$; PPARγ$^{f/f}$ per RGZ, $n = 5$; CD PPARγ KO per vehicle, $n = 4$; CD PPARγ KO group, $n = 4$. (*b*) Plasma aldosterone levels in PPARγ$^{f/f}$ and CD PPARγ KO mice after RGZ treatment. $n = 4$ in each group. (*c*) Determination of plasma volume PPARγ$^{f/f}$ and CD PPARγ KO mice by the Evans blue technique. PPARγ$^{f/f}$ per vehicle, $n = 5$; PPARγ$^{f/f}$ per RGZ, $n = 6$; CD PPARγ KO per vehicle, $n = 4$; CD PPARγ KO group, $n = 4$.

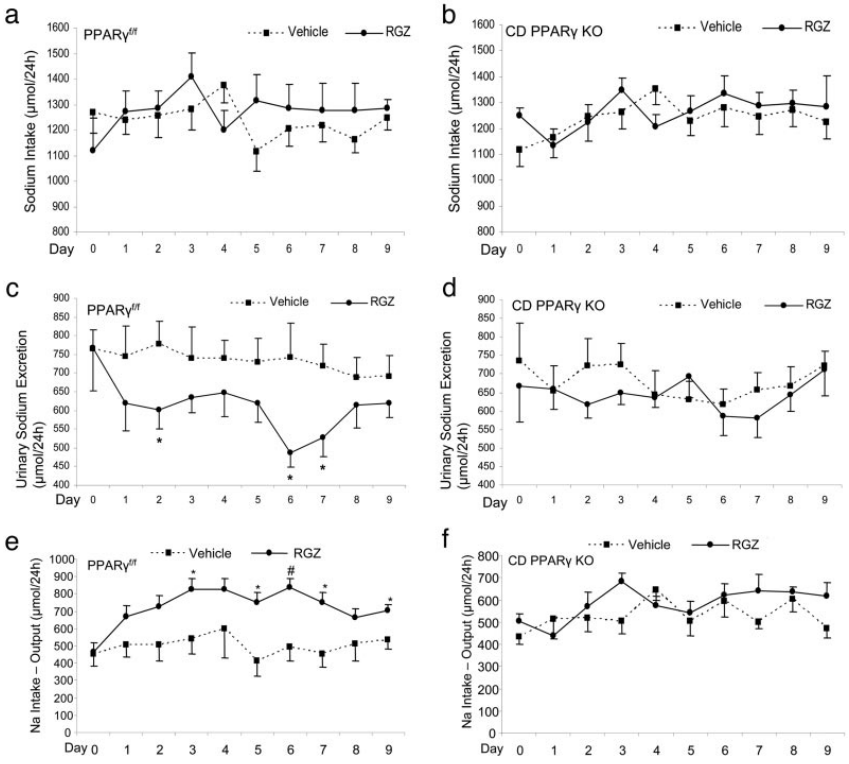

Fig. 4. Comparison of urinary sodium excretion and sodium intake between PPRA$\gamma^{f/f}$ and CD PPARγ KO mice. After a 7-day acclimation period, PPRA$\gamma^{f/f}$ and CD PPARγ KO mice were treated for 9 days with the gelled diet incorporated with or without RGZ. Shown are daily sodium intake (*a* and *b*), urinary sodium excretion (*c* and *d*), and sodium balance (intake–output) (*e* and *f*). $n = 9$ in each group. *, $P < 0.05$ vs. vehicle; #, $P < 0.001$ vs. vehicle at the corresponding time point.

allele, detected as 1,419-bp band, was present in Glom, PCT, cTAL, and mTAL, but was almost undetectable in the CD (Fig. 1*c*). Using lectin-coated Dynabeads, we isolated CD cells from PPAR$\gamma^{f/f}$ and CD PPARγ KO mice. The PPAR$\gamma^{f/f}$ cells expressed abundant PPARγ protein mostly in the nucleus, as assessed by immunocytochemistry. In contrast, PPARγ protein expression in the PPARγ KO cells was markedly reduced (Fig. 1*d*).

Comparison of Body Weights. TZDs induce body weight gain in both humans and rats as a result of fluid retention. Therefore, we monitored changes in body weights in PPAR$\gamma^{f/f}$ and CD PPARγ KO mice after a 9-day RGZ treatment. We found that RGZ induced a gradual and significant increase in body weights in the floxed mice as compared with the untreated floxed animals (2.74 ± 0.25 vs. $1.05 + 0.16$ g on day 9, $P < 0.05$). In contrast, body weight gains between RGZ-treated and untreated CD PPARγ KO mice were not significantly different (0.90 ± 0.25 vs. 0.81 ± 0.19 g on day 9, $P > 0.05$) (Fig. 2).

Comparison of Plasma Volumes. We monitored Hct changes in PPAR$\gamma^{f/f}$ and CD PPARγ KO mice before and after RGZ treatment. Blood samples were collected from the sphenous vein in awake animals for determination of Hct. RGZ treatment consistently induced a fall of Hct from $51.0 \pm 2.3\%$ to $45.0 \pm 1.2\%$ ($P < 0.01$) in PPAR$\gamma^{f/f}$ mice (Fig. 3*a*). A trend for a reduction of Hct was seen in CD PPARγ KO mice but did not reach statistical significance.

Plasma aldosterone levels are widely used as a reliable index of plasma volume. Thus we compared RGZ-induced changes in plasma aldosterone levels between the two strains of mice. We observed a significant fall of plasma aldosterone levels in PPAR$^{f/f}$ mice after RGZ treatment, in contrast to the insignificant changes in CD PPARγ KO mice (Fig. 3*b*). The pattern of changes in plasma aldosterone levels was similar to those in Hct levels.

To confirm the results obtained with indirect measurements, we used the Evans blue technique to accurately measure plasma volume. The Evans blue technique is widely used to determine plasma volume in humans (23, 24), dog (25), and rat (26). Plasma volume in untreated PPAR$^{f/f}$ mice was 62.5 ± 1.6 μl per gram, which approximates the value of 54 ± 7 ml/kg in dog (25). A 9-day RGZ treatment induced a 32.2% increase in plasma volume in PPAR$\gamma^{f/f}$ mice. In the basal state, CD PPARγ KO mice had a normal plasma volume that was not significantly different from the floxed controls. However, the KO mice had a significantly reduced plasma volume expansion induced by RGZ (Fig. 3*c*).

Comparison of Sodium Balance. We performed metabolic studies to determine sodium intake and excretion in PPAR$\gamma^{f/f}$ and CD PPARγ KO mice before and after RGZ treatment. After RGZ treatment, PPAR$^{f/f}$ mice had unchanged sodium intake but a significant reduction of urinary sodium excretion that peaked at day 6 and returned to normal at day 8; CD PPARγ KO mice did not exhibit significant changes in either sodium intake or urinary sodium excretion (Fig. 4 *a–d*). Sodium balance was further determined by subtracting output from intake. RGZ treatment induced a positive sodium balance in the control mice but not in CD PPARγ KO mice (Fig. 4 *e* and *f*).

Comparison of Sodium Transport in the Primary Culture of CD Cells. We attempted to address the cellular mechanism of differences in the RGZ-induced plasma volume expansion between PPAR$^{f/f}$ and CD PPARγ KO mice. Therefore, we established primary cultures

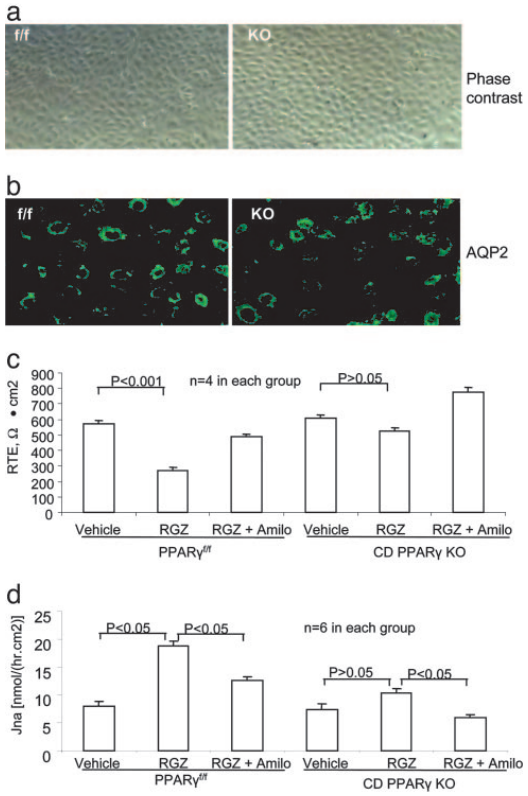

Fig. 5. Comparison of sodium transport between the cultured CD cells derived from PPARγ$^{f/f}$ and CD PPARγ KO mice. (*a*) Phase-contrast micrograph of confluent CD cells derived from PPARγ$^{f/f}$ and CD PPARγ KO mice. (*b*) AQP2 immunocytochemistry showing AQP2 expression in the unstimulated control and CD PPARγ KO cells. (*c*) Changes of transepithelial resistance (RTE) in the control and CD PPARγ KO cells after RGZ treatment. (*d*) Changes in ^{22}Na flux in the control and PPARγ KO cells after RGZ treatment.

of CD cells derived from the two strains of mice for a parallel examination of sodium transport in response to RGZ treatment. We used biotinylated Dolichos biflorus agglutinin-coated Dynabeads to isolated CD cells. These cells exhibited epithelial cell like morphology (Fig. 5*a*). In the basal state, they expressed abundant AQP2 mostly in cytoplasm as assessed by immunocytochemistry (Fig. 5*b*). Cell morphology between the control and CD PPARγ KO cells was not obviously different nor was the expression of AQP2. For measurements of sodium transport, the CD cells were subcultured onto permeable filter supports. Measurement of ^{14}C-inulin leak across the monolayers was performed to determine whether confluent cells were a tight monolayer. The leak of ^{14}C-inulin from the apical to basal was 0.46 ± 0.12% and 0.87 ± 0.24% in the period of 10 min and 1 h, respectively. There were no differences detected between the control and PPAR KO cells (0.58 ± 0.21% vs. 0.35 ± 0.01% at 10 min, and 0.90 ± 0.35% vs. 0.83 ± 0.37% at 1 h, respectively, $P > 0.05$). Exposure of the control cells to 1 μM RGZ for 24 h significantly reduced transepithelial resistance in an amiloride-sensitive manner, suggesting activation of epithelial sodium channel (ENaC)-mediated sodium transport (Fig. 5*c*). In contrast, the same RGZ treatment had no obvious effect on transepithelial resistance in the CD PPARγ KO cells. Similarly, the RGZ treatment induced a significant increase in transepithelial ^{22}Na flux in the control cells in an amiloride-sensitive manner. The RGZ-induced changes in ^{22}Na flux were significantly blocked in the PPARγ KO cells.

Discussion

The PPARγ activators, TZDs, are insulin-sensitizing agents that improve insulin sensitivity as well as parameters of blood pressure and endothelial function. Currently, two TZDs, RGZ and pioglitazone, are being widely used for the treatment of type II diabetes as efficient insulin sensitizers alone or in combination with other antidiabetic agents such as metformin, sulfonylureas, or insulin. However, these drugs are associated with significant fluid retention as the most common and serious side effect. The current study describes a Cre-Loxp approach to testing the role of CD PPARγ in TZD-induced fluid retention. To achieve CD-specific deletion of PPARγ, we used the mouse AQP2 promoter to drive Cre expression specifically in the CD. Specific recombination in the CD was validated by PCR on microdissected nephron segments. A 9-day RGZ treatment consistently increased body weight in PPARγ$^{f/f}$ but not in CD PPARγ KO mice. After RGZ treatment, PPARγ$^{f/f}$ mice exhibited severe plasma volume expansion, as reflected by significant decreases in Hct and plasma aldosterone levels, and increases in plasma volume, as measured by the Evans blue technique. In contrast, the RGZ-induced plasma volume expansion was remarkably blunted in CD PPARγ KO mice.

It is well documented that TZD-induced edema is caused by a positive sodium balance (intake > excretion). In this regard, Song *et al.* (27) reported that chronic 3-day administration of RGZ to Sprague–Dawley rats significantly reduced urine volume (by 22%) and sodium excretion (by 44%). Because electrolyte and water metabolism are largely maintained at the renal level, it is reasonable to speculate that renal mechanisms will play a major role in TZD-induced fluid retention. Within the kidney, PPARγ is highly expressed in the renal medullary CD, with lower expression levels in glomeruli, proximal tubules, and microvasculature, as demonstrated by both RT-PCR and microdissection and by *in situ* hybridization techniques (17, 18, 28). This distribution pattern suggests the possibility that local activation of PPARγ in the CD may stimulate sodium reabsorption and account for the fluid retention. This notion is supported by several lines of direct and indirect evidence from previous studies. First, in a cultured human cortical CD cell line, PPARγ agonists increase levels of cell surface ENaCα, paralleled by stimulation of gene expression of serum and glucocorticoid regulated kinase 1 (SGK1), a key mediator of aldosterone activation of ENaC (29). Second, a PPARγ ligand, GI262570, increased expressions of ENaCα, SGK1, and Na-K-ATPaseα in the renal medulla (26). Finally, GI262570 caused sodium retention but did not affect glomerular filtration rate, renal plasma flow, and renal filtration fraction (30, 31), indirectly supporting the local action of TZDs. In line with these observations, we report that RGZ-induced plasma volume expansion was significantly blunted in PPARγ KO mice. Taken together, the observations from these previous along with our current studies provide solid evidence supporting a role for the distal nephon in fluid retention associated with TZDs.

Compared with control (PPARγ$^{f/f}$) mice, CD PPARγ KO mice exhibited a significantly blunted response to RGZ, as revealed by the extent of fluid retention; however, they still showed trends in changes in Hct, aldosterone, and plasma volume. The reason for the residual responses remaining in PPAR KO mice is unclear. One possibility is that this residual response may be due to incomplete PPARγ deletion in the CD. However, the nearly complete absence of PCR products derived from the unrecombinant allele from the inner medulla and the CD of CD PPARγ KO mice does not support this possibility. Apart from the distal nephron, other sites of action of TZDs may also contribute to fluid retention. PPARγ agonists decrease lithium clearance in humans, suggesting some stimulation

of reabsorption in the proximal tubules (32). Several proximal tubule transporters including sodium hydrogen exchanger-3 undergo changes in gene expression in response to RGZ treatment (27). However, these observations are not supported by the finding that PPARγ mRNA is not detected in proximal tubules (18). PPARγ is expressed in the vascular system (33), such as in endothelial cells (34, 35), vascular smooth muscle cells (36), and monocyte/macrophages (37, 38), where TZDs may affect vascular function, leading to edema. In line with this notion, PPARγ activators RGZ and pioglitazone prevent hypertension as well as the vascular changes induced by angiotensin II infusion (39). RGZ also lowers blood pressure in normotensive rats (27). A recent study by Ryan *et al.* (40) showed that TZDs exerted a direct vasodilatory effect in isolated carotid artery but through PPARγ-independent mechanisms. Overall, other sites than the distal nephron, such as the vasculature, may still contribute to the TZD-induced fluid retention; however, any contribution from these sites is unlikely to be significant.

It is conceivable that the TZD-induced fluid retention is mediated by a PPARγ-dependent activation of sodium transport in the distal nephron. Therefore, primary cultures of CD cells derived from $PPAR\gamma^{f/f}$ and CD PPARγ KO mice were established for parallel examination of sodium transport in response to RGZ treatment. In control cells, RGZ treatment had a direct stimulatory effect on sodium transport, as assessed by both transepithelial resistance and transepithelial ^{22}Na flux. In sharp contrast, the RGZ effect was almost completely blocked in the CD PPARγ KO cells. These observations strongly suggest that the stimulatory effect of RGZ on sodium transport is mediated by PPARγ, ruling out nonspecific mechanisms. It is evident that PPARγ functions as a positive regulator of sodium transport process in the distal nephron, which likely underlies TZD-induced fluid retention.

Besides addressing the mechanism of TZD-induced fluid retention, the data presented in the present study strongly support the notion that PPARγ may function as a physiological regulator of sodium transport process in the distal nephron. In cases of modest changes in sodium intake, CD PPARγ KO mice do not exhibit signs of altered balance of electrolytes and water. These findings suggest that PPARγ in the distal nephron is not required for the maintenance of fluid homeostasis in the normal physiological state. However, this does not rule out the possibility that PPARγ may play a role under more stressful conditions with significant changes in salt or water intake. If PPARγ serves as a physiological regulator of the CD function, a question arises as to what is the endogenous ligand for the nuclear receptor. 15-deoxy-Delta(12,14)-prostaglandin J_2 (15d-PGJ_2), a product of prostaglandin D_2, is an effective activator of PPARγ in several *in vitro* systems (41, 42). Despite some evidence for endogenous biosynthesis of 15d-PGJ_2 in a number of cell types (43, 44), it remains uncertain whether 15d-PGJ_2 is produced in the kidney in a sufficient amount to act as an effective endogenous ligand for PPARγ *in vivo*.

Conclusion

The present study generated mice with CD-specific deletion of PPARγ by genetic cross between PPARγ floxed mice with transgenic mice expressing Cre under the control of the mouse AQP2 promoter. After chronic treatment with the PPARγ ligand, control mice developed severe volume expansion in sharp contrast to the significantly blunted response in CD PPARγ KO mice. Overall, our study provides insight into TZD-induced edema and also suggests an area of research concerning PPARγ-dependent mechanisms for the control of fluid homeostasis.

We thank Mark A. Knepper (National Heart, Lung, and Blood Institute, National Institutes of Health, Bethesda, MD) for providing the AQP2 antibody. This work was supported by National Institutes of Health Grants RO-1 HL079453, RO-1 DK066592, and K01 DK064981 (to T.Y.).

1. Cheng-Lai, A. & Levine, A. (2000) *Heart Dis.* **2,** 326–333.
2. Parulkar, A. A., Pendergrass, M. L., Granda-Ayala, R., Lee, T. R. & Fonseca, V. A. (2001) *Ann. Intern. Med.* **134,** 61–71.
3. Haffner, S. M., Greenberg, A. S., Weston, W. M., Chen, H., Williams, K. & Freed, M. I. (2002) *Circulation* **106,** 679–684.
4. Hirsch, I. B., Kelly, J. & Cooper, S. (1999) *Arch. Intern. Med.* **159,** 1811.
5. Fuchtenbusch, M., Standl, E. & Schatz, H. (2000) *Exp. Clin. Endocrinol. Diabetes* **108,** 151–163.
6. Thomas, M. L. & Lloyd, S. J. (2001) *Ann. Pharmacother.* **35,** 123–124.
7. Nesto, R. W., Bell, D., Bonow, R. O., Fonseca, V., Grundy, S. M., Horton, E. S., Le Winter, M., Porte, D., Semenkovich, C. F., Smith, S., *et al.* (2003) *Circulation* **108,** 2941–2948.
8. Bando, Y., Ushiogi, Y., Okafuji, K., Toya, D., Tanaka, N. & Fujisawa, M. (1999) *J. Int. Med. Res.* **27,** 53–64.
9. Walker, A. B., Naderali, E. K., Chattington, P. D., Buckingham, R. E. & Williams, G. (1998) *Diabetes* **47,** 810–814.
10. Yoshimoto, T., Naruse, M., Nishikawa, M., Naruse, K., Tanabe, A., Seki, T., Imaki, T., Demura, R., Aikawa, E. & Demura, H. (1997) *Am. J. Physiol.* **272,** E989–E996.
11. Hosokawa, M., Tsukada, H., Fukuda, K., Oya, M., Onomura, M., Nakamura, H., Kodama, M., Yamada, Y. & Seino, Y. (1999) *J. Pharmacol. Exp. Ther.* **290,** 1080–1084.
12. Keller, H., Mahfoudi, A., Dreyer, C., Hihi, A. K., Medin, J., Ozato, K. & Wahli, W. (1993) *Ann. N.Y. Acad. Sci.* **684,** 157–173.
13. Schoonjans, K., Staels, B. & Auwerx, J. (1996) *Biochim. Biophys. Acta* **1302,** 93–109.
14. Dreyer, C., Krey, G., Keller, H., Givel, F., Helftenbein, G. & Wahli, W. (1992) *Cell* **68,** 879–887.
15. Braissant, O., Foufelle, F., Scotto, C., Dauca, M. & Wahli, W. (1996) *Endocrinology* **137,** 354–366.
16. Gilde, A. J., van der Lee, K. A., Willemsen, P. H., Chinetti, G., van der Leij, F. R., van der Vusse, G. J., Staels, B. & van Bilsen, M. (2003) *Circ. Res.* **92,** 518–524.
17. Guan, Y., Zhang, Y., Davis, L. & Breyer, M. D. (1997) *Am. J. Physiol.* **273,** F1013–F1022.
18. Yang, T., Michele, D. E., Park, J., Smart, A. M., Lin, Z., Brosius, F. C., 3rd, Schnermann, J. B. & Briggs, J. P. (1999) *Am. J. Physiol.* **277,** F966–F973.
19. Akiyama, T. E., Sakai, S., Lambert, G., Nicol, C. J., Matsusue, K., Pimprale, S., Lee, Y. H., Ricote, M., Glass, C. K., Brewer, H. B., Jr., *et al.* (2002) *Mol. Cell. Biol.* **22,** 2607–2619.
20. Ge, Y., Ahn, D., Stricklett, P. K., Hughes, A. K., Yanagisawa, M., Verbalis, J. G. & Kohan, D. E. (2005) *Am. J. Physiol.*, in press.
21. Stokes, J. B., Grupp, C. & Kinne, R. K. (1987) *Am. J. Physiol.* **253,** F251–F262.
22. Wilson, P. D., Sherwood, A. C., Palla, K., Du, J., Watson, R. & Norman, J. T. (1991) *Am. J. Physiol.* **260,** F420–F430.
23. Ross, M. G. & Idah, R. (2004) *J. Matern. Fetal Neonatal Med.* **15,** 104–108.
24. Iwasaki, K., Zhang, R., Perhonen, M. A., Zuckerman, J. H. & Levine, B. D. (2004) *Am. J. Physiol.* **287,** R1256–R1262.
25. Merrill, D. C. & Cowley, A. W., Jr. (1987) *Am. J. Physiol.* **252,** F26–F31.
26. Chen, L., Yang, B., McNulty, J. A., Clifton, L. G., Binz, J. G., Grimes, A. M., Strum, J. C., Harrington, W. W., Chen, Z., Balon, T. W., *et al.* (2004) *J. Pharmacol. Exp. Ther.* **312,** 718–725.
27. Song, J., Knepper, M. A., Hu, X., Verbalis, J. G. & Ecelbarger, C. A. (2004) *J. Pharmacol. Exp. Ther.* **308,** 426–433.
28. Guan, Y., Zhang, Y., Schneider, A., Davis, L., Breyer, R. M. & Breyer, M. D. (2001) *Am. J. Physiol.* **281,** F1036–F1046.
29. Hong, G., Lockhart, A., Davis, B., Rahmoune, H., Baker, S., Ye, L., Thompson, P., Shou, Y., O'Shaughnessy, K., Ronco, P., *et al.* (2003) *FASEB J.* **17,** 1966–1968.
30. Yang, B., Clifton, L. G., McNulty, J. A., Chen, L., Brown, K. K. & Baer, P. G. (2003) *J. Cardiovasc. Pharmacol.* **42,** 436–441.
31. Gardiner, S. M., Nunez, D. J., Baer, P. G., Brown, K. K. & Bennett, T. (2004) *J. Pharmacol. Exp. Ther.* **310,** 1226–1233.
32. Zanchi, A., Chiolero, A., Maillard, M., Nussberger, J., Brunner, H. R. & Burnier, M. (2004) *J. Clin. Endocrinol. Metab.* **89,** 1140–1145.
33. Bishop-Bailey, D. (2000) *Br. J. Pharmacol.* **129,** 823–834.
34. Inoue, I., Shino, K., Noji, S., Awata, T. & Katayama, S. (1998) *Biochem. Biophys. Res. Commun.* **246,** 370–374.
35. Satoh, H., Tsukamoto, K., Hashimoto, Y., Hashimoto, N., Togo, M., Hara, M., Maekawa, H., Isoo, N., Kimura, S. & Watanabe, T. (1999) *Biochem. Biophys. Res. Commun.* **254,** 757–763.
36. Staels, B., Koenig, W., Habib, A., Merval, R., Lebret, M., Torra, I. P., Delerive, P., Fadel, A., Chinetti, G., Fruchart, J. C., *et al.* (1998) *Nature* **393,** 790–793.
37. Chinetti, G., Griglio, S., Antonucci, M., Torra, I. P., Delerive, P., Majd, Z., Fruchart, J. C., Chapman, J., Najib, J. & Staels, B. (1998) *J. Biol. Chem.* **273,** 25573–25580.
38. Ricote, M., Li, A. C., Willson, T. M., Kelly, C. J. & Glass, C. K. (1998) *Nature* **391,** 79–82.
39. Diep, Q. N., El Mabrouk, M., Cohn, J. S., Endemann, D., Amiri, F., Virdis, A., Neves, M. F. & Schiffrin, E. L. (2002) *Circulation* **105,** 2296–2302.
40. Ryan, M. J., Didion, S. P., Mathur, S., Faraci, F. M. & Sigmund, C. D. (2004) *Hypertension* **43,** 661–666.
41. Forman, B. M., Tontonoz, P., Chen, J., Brun, R. P., Spiegelman, B. M. & Evans, R. M. (1995) *Cell* **83,** 803–812.
42. Kliewer, S. A., Lenhard, J. M., Willson, T. M., Patel, I., Morris, D. C. & Lehmann, J. M. (1995) *Cell* **83,** 813–819.
43. Bell-Parikh, L. C., Ide, T., Lawson, J. A., McNamara, P., Reilly, M. & FitzGerald, G. A. (2003) *J. Clin. Invest.* **112,** 945–955.
44. Gilroy, D. W., Colville-Nash, P. R., Willis, D., Chivers, J., Paul-Clark, M. J. & Willoughby, D. A. (1999) *Nat. Med.* **5,** 698–701.

CHAPTER 3

THE MECHANISM BY WHICH PPARγ AGONISTS INDUCED FLUID RETENTION

Introduction

Peroxisome proliferator-activated receptor gamma (PPARγ) is a nuclear receptor and a member of the NR1C subgroup that includes PPARα and PPARδ. These receptors heterodimerize with the retinoid X receptor (RXR) and bind to PPAR responsive elements in the regulatory region of target genes. PPARγ is most abundantly expressed in the adipose tissue where it plays a pivotal role in driving adipocyte differentiation and maintaining adipocyte specific functions, such as lipid storage in the white adipose tissue and energy dissipation in the brown adipose tissue (1-6). In addition, PPARγ is a key regulator of glucose metabolism through improvement of insulin sensitivity. This insulin sensitizing activity affords the therapeutic potential of PPARγ activation in management of hyperglycemia and insulin resistance in type 2 diabetes. Recently, growing evidence suggests that PPARγ possesses anti-inflammatory property, representing additional benefits in limiting atherosclerosis or other inflammatory processes directly or indirectly related to diabetes (7). Among synthetic

compounds that activate PPARγ, thiazolidinediones (TZDs), including Actos (pioglitazone) and Avandia (RGZ), display remarkable enhancement of insulin action and improvement of glycemic control in patients with type 2 diabetes (8,9).

Despite their proven efficacy, TZDs possess a number of deleterious side effects. Fluid retention has emerged as the most common and serious side effect of TZDs(10-12). The incidence of TZD-induced fluid retention ranges from 7% in monotherapy and to as high as 15% when combined with insulin (10-12). The fluid retention is often presented as peripheral edema, which can progress into pulmonary edema and congestive heart failure. TZD use leads to a 6-7% increase in blood volume in healthy volunteers (13,14). Global awareness of this side effect has increased as a result of the growing number of reported cases. American Heart Association and American Diabetes Association jointly issued a Consensus Statement commenting on the safety of TZD as related to edema (15). Although multiple factors may be involved, increased fluid reabsorption in the distal nephron appears to be a major determinant of TZD-induced fluid retention. In this regard, PPARγ expression is predominatly expressed in the collecting duct (16,17). More importantly, conditional deletion of PPARγ in the collecting duct remarkably attenuated RGZ- or pioglitazone-induced body weight gain and plasma volume expansion found in wild type mice (18,19).

Transcellular transport of Na^+ in the CD is mainly mediated by ENaC, which is comprised of three subunits, α, β, and γ. These proteins are vital to day-to-day adjustment of urinary Na^+ excretion and are subjected to hormonal regulation by aldosterone, insulin, and vasopressin (20-22). A number of studies

examined the possibility of PPARγ regulation of ENaC and yielded conflicting results (19,23,24). The goal of the present study is to examine involvement of ENaC in PPARγ-dependent stimulation of ion transport.

Materials and methods

Materials

Amiloride and epidermal growth factor (EGF) were purchased from Sigma. DMEM medium was from American Type Culture Collection (ATCC) (Manassas, VA). Snapwell permeable supports were from Corning Incorporated (Corning, NY). Collagen type I was from Worthington Biochemical Corp. (Lakewood, NJ).

Animals

C57/BL6 mice were purchased from Jackson Laboratory and were used as wild type mice. Collecting duct-specific PPARγ knockout (CD PPARγ KO) mice were generated by crossing PPARγ floxed mice with mAQP2-Cre mice and were used only in the ion substitution experiments. All mice were maintained in a temperature-controlled barrier facility with a 12 h/12 h light/dark cycle and were given free access to standard laboratory chow and tap water. All protocols employing mice were conducted in accordance the principles and guidance of Institutional Animal Care and Committee at the University of Utah.

RGZ treatment

RGZ was incorporated into a chow-based diet (LabDiet Rodent Chow 5001; Purina Mills, St. Louis, MO) at a level of 320 mg/kg diet. The gelled diets were made by melting agar (1% by weight) in water (65%), cooling and adding the drug (0.1%), and ground chow (33.9%), and NaCl (0.5%). The final content of NaCl became 0.8%. The same gelled diets without the drug served as controls. Adult PPARγ$^{f/f}$ and CD PPARγ KO mice (3~4-month-old) were acclimatized to metabolic cages (Hatteras Instruments) and the control diet for 7 days. The numbers of males and females were roughly even in each group. After the 7-day acclimation period, PPARγ$^{f/f}$ and CD PPARγ KO mice were placed on the gelled diet with or without RGZ, for 9 days. At the end of experiments, under anesthesia, kidneys are harvested and processed for evaluation of the states of sodium transporters including various isoforms of ENaC and Na-K-ATPase. Gene expression levels of the transporters will be determined by qRT-PCR.

Cell culture

Mice were killed by cervical dislocation and kidneys were quickly removed under sterile conditions. The renal inner medulla was dissected, minced, and digested for 60 min in 10 ml of DMEM medium containing 0.2% collagenase type I, 0.2% hyaluronidase, and 0.025% trypsin-EDTA at 37 ºC with shaking. After incubation, 20 ml of sterile distilled water was added for 20 min to lyse cells other than collecting duct cells by osmotic shock (100 mOsm/kg·H_20). Cells were then centrifuged at 1,000 rpm for 5 min, the supernatant was discarded, and the pellet

resuspended in the modified medium (DMEM, 10% fetal bovine serum, 20 ng/ml, and 100 units/ml penicillin G-streptomycin sulfate). Cells were seeded onto semipermeable 12-mm-diameter Snapwell membranes for electrophysiological studies. After the cells reached confluence, usually in 10 days, the cells were incubated in serum-free media for at least 4 h before experiments. The cell monolayers were confirmed to be confluent by development of high resistance. The short-circuit current (Isc) and the transepithelial voltage (Vte) were determined by using VCC600 voltage clamp apparatus (Physiologic instruments, San Diego, CA, USA). The transepithelial resistance (TER) was measured by using EVOM epithelial volt-ohm-meter and a set of two stick STX electrodes (World Precision Instruments, Sarasota, Fl, USA). Only the cell monolayers reaching the resistance >1000 $\Omega.cm^2$ were used for electrophysiological studies.

Electrophysiological transepithelial measurements

Snapwell semipermeable membranes containing confluent cell monolayers were mounted in an Ussing chamber (Physiologic instruments, San Diego, CA, USA) and both surfaces of the cell monolayer were bathed in completed media (NaCl, 120 mM; KCl, 4.2 mM; NaHCO3, 34 mM; $MgCl_2$, 0.3 mM; Na_2HPO_4, 1mM; $MgSO_4$, 0.4 mM; $CaCl_2$, 1.05 mM; glucose, 20 mM) maintained at 37 ºC and equilibrated in 5% CO_2-95% O_2 to keep pH at 7.4. The transepithelial voltage was clamped at zero using VCC600 voltage clamp apparatus, and then the short-circuit current (Isc) was recorded using Ag-AgCl electrode in agar brides after 60 min equilibration period. Positive Isc reflects the

active transport of cation (Na^+) from apical side to basolateral side media or transport of anion (Cl^-) from apical to basolateral side of media.

qRT-PCR

Total RNA was isolated from primary IMCD cells using TRIzol. One microgram of total RNA was denatured at 65°C for 5 min, and cDNA synthesis was then performed at 42°C for 1 h using Superscript reverse transcriptase (BRL, Gaithersburg, MD). Oligonucleotides were designed using Primer3 software (available at http://frodo.wi.mit.edu/cgi-bin/primer3/primer3_www.cgi). The sequences of the primers were as follows: α-ENaC, 5'-gagagcctggcacagagagg-3' (sense), 5'-cggctttcacgccctcttg-3' (antisense); β-ENaC , 5'-tttggcttccagcctgacaca-3'(sense), 5'-cgggatgggcagagtctgtt-3'(antisense); γ-ENaC,5'-ccttcaagctgagcgaacct-3'(sense),5'-gatgtttgtgacgggcacatc-3'(antisense). qPCR amplification was performed using the SYBR Green Master Mix (Applied Biosystems) and the Prism 7500 Real-Time PCR Detection System (Applied Biosystems). Cycling conditions were 95°C for 10 min, followed by 40 repeats of 95°C for 15 s and 60°C for 1 min.

Data analysis

Data are summarized as mean $\pm$ SE. Statistical analysis was performed using one-way ANOVA or student paired t-test as appropriate.

Results

RGZ and PPARγ knockout do not affect ENaC expression in renal inner medulla

To examine the effect of PPARγ agonists on ENaC expression, we performed RGZ and vehicle treatment on wild type (WT) and CD PPARγ KO mice (KO) for 9 days. Inner medullas were dissected from mouse whole kidneys. mRNA expression of the 3 ENaC subunits (α-, ß-, and γ-) was subsequently determined by using qRT-PCR. Figure 3.1 summarizes the mRNA expression of the ENaC α, ENaCß, ENaCγ subunits in WT and CD PPARγ KO inner medullas. Nine days RGZ treatment had no effect on ENaC α, ENaCß expression. There is a reduced trend on ENaCγ expression but it did not reach statistical significance. We also did not observe the ENaC expression difference between KO-Vehicle and WT-Vehicle groups. These findings demonstrate that RGZ and PPARγ knockout do not affect ENaC expression in renal inner medulla.

RGZ inhibits ENaC activity and expression in primary culture cells

ENaC represents the major route of transcellular transport in the CD and is reported to be variably regulated by PPARγ. We performed the Ussing chamber technique to examine the effect of RGZ on ENaC activity and expression in primary cultures of mouse IMCD cells. The confluent IMCD cell monolayers were fasted with serum-free media for 4 h, followed by exposure to 1 μM RGZ for 24 or 48 h. Electromicroscopy confirmed formation of the tight junction that was not obviously affected by RGZ treatment (data not shown). The

amiloride-sensitive currents were used as an index of ENaC activity. The ENaC activity was unaffected at 24 h but was significantly reduced at 48 h of RGZ treatment (Fig.3.2). mRNA expression of the 3 ENaC subunits (α-, ß-, and γ-) was subsequently determined by using qRT-PCR. The pattern of changes in mRNA expression in response to RGZ treatment was similar among the 3 ENaC subunits. At 24 h, the expression level in the RGZ group tended to be lower than in the control group but this difference did not reach statistical significance (Fig. 3.3A). The difference became significant at 48 h (Fig. 3.3B).

RGZ reduces the TER

The changes in the TER are inversely related epithelial transport rate with low TER typically reflecting increased ion transport across the cell monolayer. We examined the effect of RGZ on the TER in primary cultures of IMCD cells. The exposure of IMCD cell monolayers to 1 μM RGZ decreased the TER by 50% ($P < 0.01$) at 24 h and by 70% at 48 h ($P < 0.01$) (Fig. 3.4). Since ENaC was suppressed, the reduction of the TER seemed to indicate an alternative route of increased ion flux.

Discussion

PPARγ is a ligand-activated transcriptional factor that heterodimerizes with RXR to regulate expression of a wide range of target genes involved in adipogenesis, glucose uptake, and inflammatory response. Recently, renal action of PPARγ has received fresh attention particularly due the relevance to TZD-

induced fluid retention, the major side effect of the promising antidiabetes drugs. Within the kidney, PPARγ is expressed predominantly in the CD, with low or absent levels of expression in proximal tubule and thick ascending limb, as assessed by both microdissection coupled with RT-PCR and in situ hybridization techniques (16,17). Thus, the CD is a likely target site for renal action of PPARγ. Conditional deletion of PPARγ in the CD in mice completely abolished or significantly attenuated RGZ-and pioglitazone-induced body weight gain and plasma volume expansion. These studies have identified a PPARγ-dependent pathway in the control of fluid reabsorption in the distal nephron which is essential for fine-tuning adjustment of urinary excretion of water and electrolytes. These findings are of clinical importance for understanding pharmacology of the antidiabetes drugs and may also be of physiological relevance based on the existence of a number of endogenously produced products that may act on PPARγ in the CD; most of these products are lipid metabolites, including nitrated free fatty acids (25,26), 15-deoxy-delta(12,14)-prostaglandin J_2 (15d-PGJ_2) (27,28), and lysophosphatidic acid (31). Therefore, it is critically important to understand the mechanism by which PPARγ regulates distal tubular fluid reabsorption.

The aim of the present study was to perform RGZ treatment on WT and KO mice and electrophysiological studies on primary cultures of CD cells to evaluate involvement of the ENaC in RGZ-induced stimulation of ion transport. Data shows RGZ and PPARγ knockout do not affect ENaC expression in renal inner medulla. There is a big standard deviation in each group in this in vivo

experiment, but ENaCγ expression still shows a reduced trend after RGZ treatment which is consistent with the results in primary cultures of CD cells. We found that RGZ treatment time-dependently inhibited amiloride-sensitive Isc, a measure of ENaC activity. The effect was not detectable until 48 h, suggesting a slow process. This finding was further confirmed at mRNA levels. At 48 h, RGZ treatment consistently suppressed mRNA expression of all ENaC subunits (α-, ß- and γ-). Given ENaC being the major Na^+ transporter on the apical membrane of the CD, these findings indicate that PPARγ may inhibit transcellular Na^+ transport. Despite the inhibition of transcellular Na^+ transport, the TER was consistently reduced following RGZ treatment, indicating an alternative route of increased ion transport.

ENaC was initially considered as a possible target of PPARγ in the CD cells. This possibility was first suggested by the study of Hong et al. showing a translocation of α-ENaC accompanied with an upregulation of SGK1 mRNA and activity in cultured human CCD cells after a 4-h exposure to PPARγ agonists (30). Subsequently, in IMCD cells, pioglitazone treatment was shown to rapidly induce γ-ENaC mRNA expression without affecting expression of α-, and ß-ENaC subunits (19). Recently, evidence suggests that PPARγ agonist treatment may induce alteration in banding patterns of renal γ-ENaC protein which were described as activating cleavage (31,32). However, emerging evidence argues against ENaC as a molecular target of PPARγ. First, none of the 3 ENaC subunits exhibited major changes in renal mRNA expression in response to a 2- or 4-day PPARγ agonist treatment in vivo (24). Second, in various CD cell lines,

PPARγ agonists failed to enhance basal or insulin-stimulated Isc (23). Third, and more importantly, CD-specific gene inactivation of α-ENaC in the mouse does not attenuate RGZ-induced body weight gain or plasma volume expansion, virtually ruling out involvement of ENaC (33). Along this line, the present study found no evidence of RGZ-induced increases in ENaC activity or expression in primary CD cells, similar to the study in CD cell lines (23). Interestingly, we found that RGZ treatment time-dependently inhibited ENaC activity and mRNA expression in primary CD cells. In the Nofziger et al. study, a similar inhibitory effect of PPARγ agonist on Isc was noticed only in M1 but not the A6 or mpkCCDc14 cell lines and also with one PPAR agonist GW7845 but not the other (pioglitazone). The inconsistent results may be related to the short time course of drug treatment (18-24 h) used in the previous study (23). Indeed, we found that the inhibition did not occur until 48 h of RGZ treatment. The mechanism by which PPARγ suppresses ENaC expression in renal CD cells still remains elusive. A seminal study by Pascual et al. demonstrates that PPARγ-dependent transcriptional suppression of inflammatory response genes in mouse macrophages involves ligand-dependent SUMOylation of the PPARγ ligand-binding domain and subsequent recruitment of nuclear receptor corepressor (NCoR)-histone deacetylase-3 (HDAC3) complexes on inflammatory gene promoters (34). Future studies are needed to determine whether a similar mechanism may underlie PPARγ-induced repression of ENaC expression in renal CD cells.

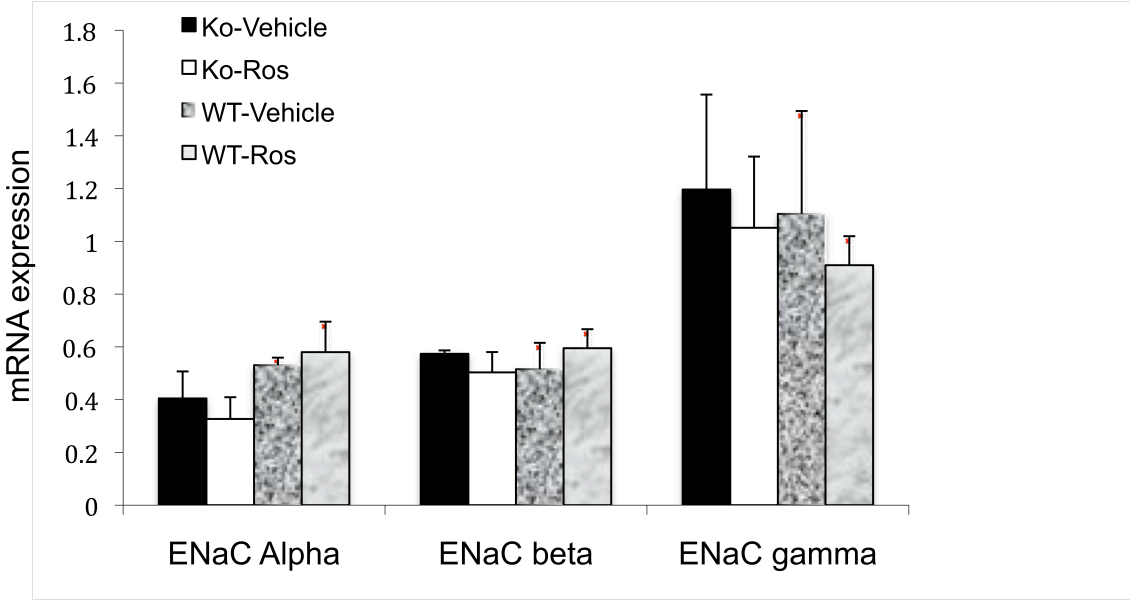

Fig. 3.1. Effect of RGZ on ENaC mRNA expression in renal inner medulla of wild type (WT) and CD PPARγ KO mice (KO). The WT and KO mice were treated with RGZ and Vehicle for 9 days. mRNA expression of α-, β-, and γ-ENaC was determined by qRT-PCR and normalized by β-actin. Data are mean ± SE. N = 4 per group.

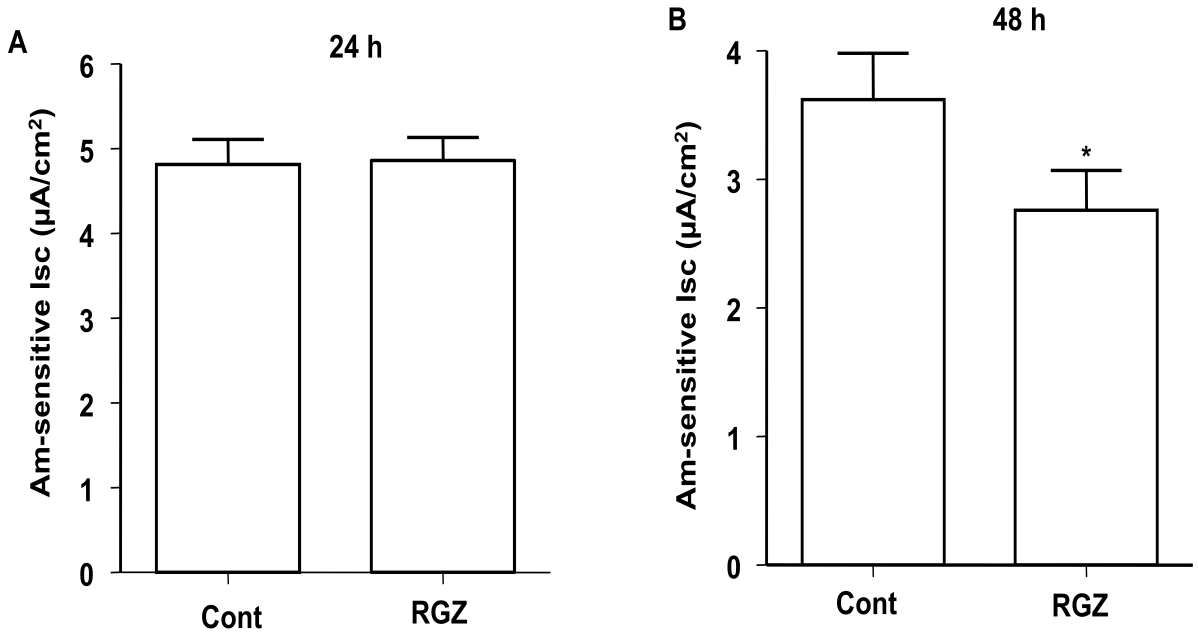

Fig.3.2. Effect of RGZ on amiloride-sensitive Isc in primary IMCD cells. The confluent cell monolayers were fasted with serum-free media for 4 h, followed by treatment with vehicle or 1 μM RGZ for 24 h (A) or 48 h (B). At the end of the experiments, the Isc was measured in the absence or presence of 100μM amiloride. *, $P < 0.05$ vs. Control. Data are mean $\pm$ SE. N = 12 per group.

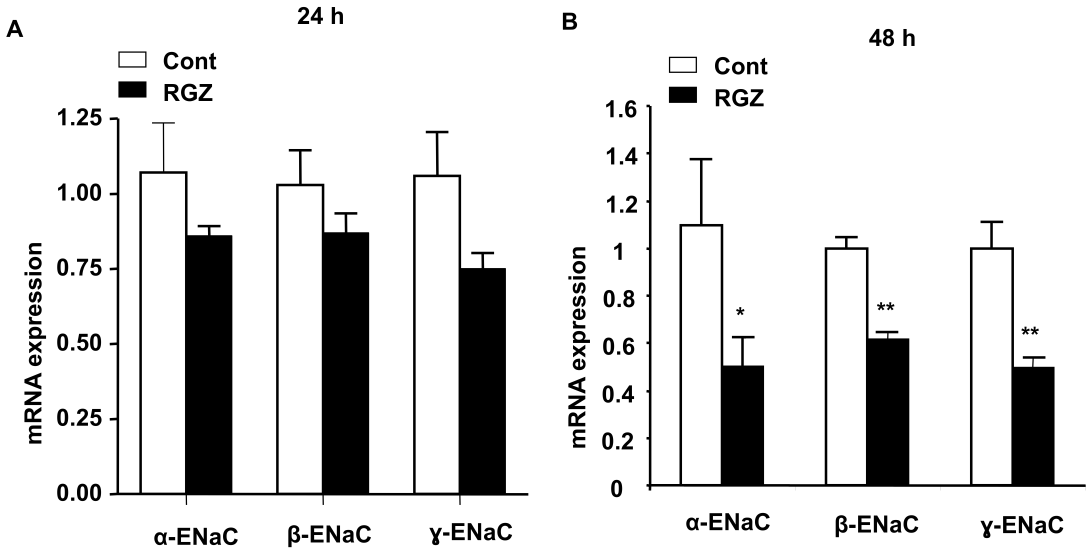

Fig. 3.3. Effect of RGZ on ENaC mRNA expression in the IMCD cells. The confluent IMCD cells were exposed to vehicle or 1 μM RGZ for 24 h (A) or 48 h (B). mRNA expression of α-, β-, and γ-ENaC was determined by qRT-PCR and normalized by β-actin. *, $P < 0.05$ and **, $P < 0.01$ vs. Control. Data are mean $\pm$ SE. N = 6 per group.

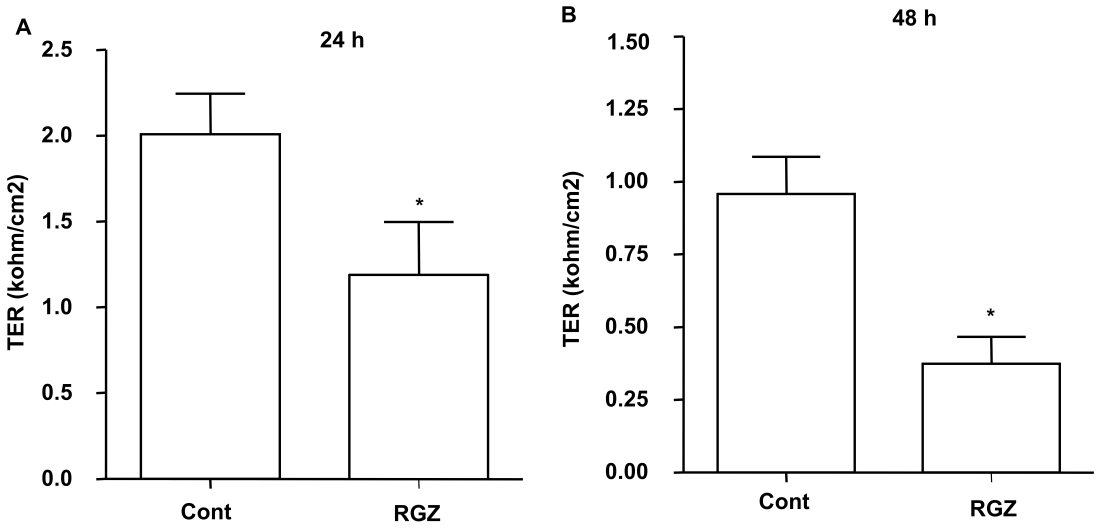

Fig. 3.4. Effect of RGZ on the TER in the IMCD cells. The confluent cell monolayers were fasted with serum-free media for 4 h, followed by treatment with vehicle or 1 μM RGZ for 24 h (A) or 48 h (B). *, $P < 0.05$ vs. Control. The data are mean $\pm$ SE. N = 12 per group.

References

1. Tontonoz P, Kim JB, Graves RA and Spiegelman BM. ADD1: a novel helix-loop-helix transcription factor associated with adipocyte determination and differentiation. *Mol Cell Biol*. 1993;13:4753-9.

2. Tontonoz P, Hu E, Graves RA, Budavari AI and Spiegelman BM. mPPAR gamma 2: tissue-specific regulator of an adipocyte enhancer. *Genes Dev*. 1994;8:1224-34.

3. Rosen ED, Walkey CJ, Puigserver P and Spiegelman BM. Transcriptional regulation of adipogenesis. *Genes Dev*. 2000;14:1293-307.

4. He W, Barak Y, Hevener A, Olson P, Liao D, Le J, Nelson M, Ong E, Olefsky JM and Evans RM. Adipose-specific peroxisome proliferator-activated receptor gamma knockout causes insulin resistance in fat and liver but not in muscle. *Proc Natl Acad Sci U S A*. 2003;100:15712-7.

5. Koutnikova H, Cock TA, Watanabe M, Houten SM, Champy MF, Dierich A and Auwerx J. Compensation by the muscle limits the metabolic consequences of lipodystrophy in PPAR gamma hypomorphic mice. *Proc Natl Acad Sci U S A*. 2003;100:14457-62.

6. Duan SZ, Ivashchenko CY, Whitesall SE, D'Alecy LG, Duquaine DC, Brosius FC, 3rd, Gonzalez FJ, Vinson C, Pierre MA, Milstone DS, and Mortensen RM. Hypotension, lipodystrophy, and insulin resistance in generalized PPARgamma-deficient mice rescued from embryonic lethality. *J Clin Invest*. 2007;117:812-22.

7. Ricote M, Li AC, Willson TM, Kelly CJ and Glass CK. The peroxisome proliferator-activated receptor-gamma is a negative regulator of macrophage activation. *Nature*. 1998;391:79-82.

8. Francis GA, Fayard E, Picard F and Auwerx J. Nuclear receptors and the control of metabolism. *Annu Rev Physiol*. 2003;65:261-311.

9. Gurnell M, Savage DB, Chatterjee VK and O'Rahilly S. The metabolic syndrome: peroxisome proliferator-activated receptor gamma and its therapeutic modulation. *J Clin Endocrinol Metab*. 2003;88:2412-21.

10. Hirsch IB, Kelly J and Cooper S. Pulmonary edema associated with troglitazone therapy. *Arch Intern Med*. 1999;159:1811.

11. Fuchtenbusch M, Standl E and Schatz H. Clinical efficacy of new thiazolidinediones and glinides in the treatment of type 2 diabetes mellitus. *Exp Clin Endocrinol Diabetes*. 2000;108:151-63.

12. Thomas ML and Lloyd SJ. Pulmonary edema associated with rosiglitazone and troglitazone. *Ann Pharmacother*. 2001;35:123-4.

13. (Pioglitazone) PIA. *Takeda Pharmaceuticals, Inc.*

14. (Rosiglitazone) PIA. *GlaxoSmithKline Pharmaceuticals.*

15. Nesto RW, Bell D, Bonow RO, Fonseca V, Grundy SM, Horton ES, Le Winter M, Porte D, Semenkovich CF, Smith S, Young LH and Kahn R. Thiazolidinedione use, fluid retention, and congestive heart failure: a consensus statement from the American Heart Association and American Diabetes Association. October 7, 2003. *Circulation*. 2003;108:2941-8.

16. Yang T, Michele DE, Park J, Smart AM, Lin Z, Brosius FC, 3rd, Schnermann JB and Briggs JP. Expression of peroxisomal proliferator-activated receptors and retinoid X receptors in the kidney. *Am J Physiol*. 1999;277:F966-73.

17. Guan Y, Zhang Y, Davis L and Breyer MD. Expression of peroxisome proliferator-activated receptors in urinary tract of rabbits and humans. *Am J Physiol*. 1997;273:F1013-22.

18. Zhang H, Zhang A, Kohan DE, Nelson RD, Gonzalez FJ and Yang T. Collecting duct-specific deletion of peroxisome proliferator-activated receptor gamma blocks thiazolidinedione-induced fluid retention. *Proc Natl Acad Sci U S A*. 2005;102:9406-11.

19. Guan Y, Hao C, Cha DR, Rao R, Lu W, Kohan DE, Magnuson MA, Redha R, Zhang Y and Breyer MD. Thiazolidinediones expand body fluid volume through PPARgamma stimulation of ENaC-mediated renal salt absorption. *Nat Med*. 2005;11:861-866.

21. Loffing J, Loffing-Cueni D, Macher A, Hebert SC, Olson B, Knepper MA, Rossier BC and Kaissling B. Localization of epithelial sodium channel and aquaporin-2 in rabbit kidney cortex. *Am J Physiol Renal Physiol*. 2000;278:F530-9.

22. Loffing J, Pietri L, Aregger F, Bloch-Faure M, Ziegler U, Meneton P, Rossier BC and Kaissling B. Differential subcellular localization of ENaC subunits in mouse kidney in response to high- and low-Na diets. *Am J Physiol Renal Physiol*. 2000;279:F252-8.

23. Masilamani S, Kim GH, Mitchell C, Wade JB and Knepper MA. Aldosterone-mediated regulation of ENaC alpha, beta, and gamma subunit proteins in rat kidney. *J Clin Invest*. 1999;104:R19-23.

24. Nofziger C, Chen L, Shane MA, Smith CD, Brown KK and Blazer-Yost BL. PPARgamma agonists do not directly enhance basal or insulin-stimulated Na(+) transport via the epithelial Na(+) channel. *Pflugers Arch*. 2005;451:445-53.

25. Chen L, Yang B, McNulty JA, Clifton LG, Binz JG, Grimes AM, Strum JC, Harrington WW, Chen Z, Balon TW, Stimpson SA and Brown KK. GI262570, a PPAR{gamma} agonist, changes electrolytes and water reabsorption from the distal nephron in rats. *J Pharmacol Exp Ther*. 2004.

27. Schopfer FJ, Lin Y, Baker PR, Cui T, Garcia-Barrio M, Zhang J, Chen K, Chen YE and Freeman BA. Nitrolinoleic acid: an endogenous peroxisome proliferator-activated receptor gamma ligand. *Proc Natl Acad Sci U S A*. 2005;102:2340-5.

28. Baker PR, Lin Y, Schopfer FJ, Woodcock SR, Groeger AL, Batthyany C, Sweeney S, Long MH, Iles KE, Baker LM, Branchaud BP, Chen YE and Freeman BA. Fatty acid transduction of nitric oxide signaling: multiple nitrated unsaturated fatty acid derivatives exist in human blood and urine and serve as endogenous peroxisome proliferator-activated receptor ligands. *J Biol Chem*. 2005;280:42464-75.

29. Forman BM, Tontonoz P, Chen J, Brun RP, Spiegelman BM and Evans RM. 15-Deoxy-delta 12, 14-prostaglandin J2 is a ligand for the adipocyte determination factor PPAR gamma. *Cell*. 1995;83:803-12.

30. Kliewer SA, Lenhard JM, Willson TM, Patel I, Morris DC and Lehmann JM. A prostaglandin J2 metabolite binds peroxisome proliferator-activated receptor gamma and promotes adipocyte differentiation. *Cell*. 1995;83:813-9.

31. McIntyre TM, Pontsler AV, Silva AR, St Hilaire A, Xu Y, Hinshaw JC, Zimmerman GA, Hama K, Aoki J, Arai H and Prestwich GD. Identification of an intracellular receptor for lysophosphatidic acid (LPA): LPA is a transcellular PPARgamma agonist. *Proc Natl Acad Sci U S A*. 2003;100:131-6.

32. Hong G, Lockhart A, Davis B, Rahmoune H, Baker S, Ye L, Thompson P, Shou Y, O'Shaughnessy K, Ronco P and Brown J. PPARgamma activation enhances cell surface ENaCalpha via up-regulation of SGK1 in human collecting duct cells. *Faseb J*. 2003;17:1966-8.

33. Song J, Knepper MA, Hu X, Verbalis JG and Ecelbarger CA. Rosiglitazone activates renal sodium- and water-reabsorptive pathways and lowers blood pressure in normal rats. *J Pharmacol Exp Ther*. 2004;308:426-433.

34. Tiwari S, Blasi ER, Heyen JR, McHarg AD and Ecelbarger CM. Time course of AQP-2 and ENaC regulation in the kidney in response to PPAR agonists associated with marked edema in rats. *Pharmacol Res*. 2008;57:383-92.

CHAPTER 4

SUMMARY AND PERSPECTIVES

Edema and fluid retention are common and serious side effects of TZD therapy, which are due to supernormal sodium reabsorbtion and consequent interstitial fluid volume expansion. We have developed a mouse model with CD-specific deletion of the PPARγ gene and characterized a novel PPARγ-dependent pathway in regulation of sodium transport in the distal nephron. Body weight gain and plasma volume expansion in response to RGZ treatment were abolished or significantly blocked by knocking out PPARγ in the CD. Our study proved that PPAR*γ* plays a critical role in systemic fluid retention through the regulation of renal sodium transport, and that the adverse effects of TZD in fluid metabolism are indeed PPAR*γ*-dependent. These findings are of clinical importance for understanding pharmacology of the antidiabetes drugs and may also be of physiological relevance based on the existence of a number of endogenously produced products that may act on PPARγ in the CD. Therefore, it is critically important to understand the mechanism by which PPARγ regulates distal tubular fluid reabsorption.

We examined the inner medulla mRNA expression of α-, ß-, and γ-ENaC in RGZ treated mice, data shows RGZ and PPARγ knockout do not affect ENaC expression in renal inner medulla. We performed electrophysiological studies on primary cultures of inner medullary collecting duct (IMCD) cells to evaluate mechanisms of rosiglitazone (RGZ)-stimulated ion transport. Following exposure to RGZ, amiloride-sensitive short-circuit current (Isc), an index of ENaC activity, was unchanged at 24 h but was significantly suppressed at 48 h, corresponding to parallel inhibition of mRNA expressions of α-, ß-, and γ-ENaC. Despite ENaC inhibition, the transepithelial resistance (TER) was significantly reduced, suggesting an alterative route of increased ion transport. In summary, these data indicates that ENaC is not critical for rosiglitazone (RGZ)-stimulated ion transport.

Recently, my colleagues in our lab examined the effect of RGZ on paracellular Na^+ and Cl^- flux. RGZ treated monolayers exhibited increases of the paracellular Cl^- flux, to a lesser extent, the paracellular Na^+ flux. In contrast, these effects were significantly blunted in the PPARγ-deficient IMCD cells. In wild type IMCD cells, together, our data suggest that PPARγ activation stimulates paracellular ion transport and inhibits ENaC in primary IMCD cells. These data suggest that the paracellular rather than transcellular route might be a primary target of PPARγ in the CD.